Structural complexity and benthic metabolism: resolving the links between carbon cycling and biodiversity in restored seagrass meadows

Theodor Kindeberg[1*], Karl M. Attard[2,3], Jana Hüller[1], Julia Müller[1], Cintia O. Quintana[2,4], Eduardo Infantes[5]

[1]Department of Biology, Lund University, Sölvegatan 37, 223 62, Lund, Sweden
[2]Department of Biology, University of Southern Denmark, 5230, Odense M, Denmark
[3]Danish Institute for Advanced Study, University of Southern Denmark, 5230, Odense M, Denmark
[4]SDU Climate Cluster, University of Southern Denmark, 5230, Odense M, Denmark
[5]Department of Biological and Environmental Sciences, University of Gothenburg, 451 78, Kristineberg, Sweden

[*]Correspondence: theo.kindeberg@gmail.com

Abstract. Due to large losses of seagrass meadows worldwide, restoration is proposed as a key strategy for increasing coastal resilience and recovery. The emergence of a seagrass meadow is expected to substantially amplify biodiversity and enhance benthic metabolism by increasing primary productivity and respiration. Yet, open questions remain regarding the metabolic balance of aging seagrass meadows and the roles benthic communities within the seagrass ecosystem play in overall metabolism.

To address these questions, we investigated a chronosequence of bare sediments, adjacent *Zostera marina* meadows of 3 and 7 years since restoration, alongside a natural meadow located within a high-temperate marine embayment in Gåsö, Sweden. We combined continuous measurements of O_2 fluxes using underwater eddy covariance with dissolved inorganic carbon (DIC) and O_2 fluxes from benthic chambers during the productive season (July). Based on the ratio between O_2 and DIC, we derived site-specific photosynthetic and respiratory quotients, enabling the conversion of eddy covariance fluxes to DIC. We assessed benthic diversity parameters as potential drivers of metabolic flux variability.

We observed high rates of gross primary productivity (GPP) spanning -18 to -82 mmol DIC m^{-2} d^{-1}, which increased progressively with meadow age. Community respiration (CR) mirrored the GPP trend, and all meadows were net heterotrophic (GPP < |CR|), with NCP ranging from 16 to 28 mmol DIC m^{-2} d^{-1}. While autotrophic biomass did not increase with meadow age, macrophyte diversity did, elucidating potential effects of niche complementarity among macrophytes on community metabolism. These findings provide valuable insights into how community composition and meadow development relate to ecosystem functioning, highlighting potential tradeoffs between carbon uptake and biodiversity.

Deleted: anticipated
Deleted: increase
Deleted: through
Deleted: ed
Deleted: of the
Deleted: three
Deleted: seven
Deleted: and
Deleted: obtained
Deleted: from which we could convert
Deleted: –
Deleted: –
Deleted: observations
Deleted: provide
Deleted: and h

1. Introduction

Climate change and concurrent biodiversity loss has motivated restoration of natural ecosystems that can contribute to climate change mitigation, adaptation and at the same time strengthen local biodiversity. One such ecosystem is seagrass meadows, which has suffered substantial losses worldwide during the last century (Waycott et al., 2009; Mckenzie et al., 2020). Due to its foundational role in structuring benthic communities, high productivity and ability to sequester large amounts of carbon, restoring previously lost meadows has been proposed as a low-regret option to address both the climate and biodiversity crises concomitantly (Duarte et al., 2013; Gattuso et al., 2018; Orth et al., 2020; Unsworth et al., 2022). Nevertheless, few studies have assessed whether both these goals are mutually attainable within the same restoration projects, or if there are tradeoffs between biodiversity conservation and carbon sequestration.

The mechanisms through which a seagrass meadow modifies carbon flows are manifold, influencing both import, export and burial of autochthonous (i.e. seagrass biomass) and allochthonous (i.e. organic matter from other sources) carbon (Duarte and Krause-Jensen, 2017). While sedimentation of allochthonous carbon is largely a passive process ultimately governed by local hydrodynamics, autochthonous carbon sequestration is coupled to the productivity of the seagrass meadow and is thus a function of its metabolic fluxes on timescales ranging from minutes to years (Smith and Key, 1975; Smith and Hollibaugh, 1993; Duarte and Cebrian, 1996). Seagrass community metabolism is comprised of gross primary productivity (GPP) and community respiration (CR) constituted by autotrophic and heterotrophic respiration. The balance between GPP and CR on a daily basis reflects the net metabolism, hereafter termed net community productivity (NCP = GPP - |CR|). The magnitude and direction of GPP, CR and NCP determine all subsequent carbon flows whereby a positive NCP (net autotrophy) equals the net carbon fixed available for remineralization, burial or export (Duarte and Krause-Jensen, 2017). Contrarily, if NCP is negative, the meadow is respiring more organic carbon than is fixed and relies on external or historic inputs of organic matter to sustain metabolism. Empirically assessing community metabolism is thus imperative to constrain a carbon budget and infer the potential net effect of a seagrass meadow on carbon sequestration.

The vast majority of metabolism studies in seagrass ecosystems to date are based on oxygen fluxes (Ward et al., 2022). Converting these fluxes into carbon currency often relies on assuming a constant stoichiometric 1:1 ratio between oxygen and dissolved inorganic carbon (O_2:DIC) fluxes which may significantly under- or overestimate actual metabolism (e.g. Barron et al., 2006; Duarte et al., 2010; Turk et al., 2015). For marine sediments, this ratio has been estimated to range between 0.8 – 1.2 on annual timescales (Glud, 2008 and references therein) but the variability is poorly constrained and likely higher in seagrass systems and on shorter timescales (Turk et al., 2015; Trentman et al., 2023). The discrepancy from a 1:1 ratio between benthic oxygen and DIC fluxes can stem from a wide range of processes, including anaerobic sediment processes, nitrate assimilation, photorespiration and differences in solubility and air-sea gas exchange rates between O_2 and CO_2 (Weiss, 1970; Trentman et al., 2023). In seagrasses, storage in tissues and transport of oxygen to roots and subsequent radial oxygen loss (ROL) can also contribute to deviations from the theoretical 1:1 relation (Borum et al., 2007; Ribaudo et al., 2011; Berg et al., 2019). Assessing carbon cycling in seagrass meadows without characterizing the marine carbonate chemistry system can thus lead to erroneous conclusions regarding their role in carbon cycling and ultimately their climate change mitigation potential.

Deleted: crisis
Deleted: the
Deleted: i
Deleted: -

Despite the growing number of seagrass restoration projects worldwide, assessments of the effect on benthic metabolism are lacking. To our knowledge, the only research effort that has specifically addressed benthic metabolism in restored seagrass was carried out in Virginia Coast Reserve, USA (Rheuban et al., 2014a), where a large-scale *Zostera marina* restoration project commenced in 2001 (Mcglathery et al., 2012). Rheuban et al. (2014a) employed a chronosequence approach comprised of a bare site and two stages of development since restoration (5 years and 11 years) and measured benthic metabolism on diel and seasonal timescales. The authors found that GPP and |CR| increased up to 25- and 10-fold, respectively with meadow age and this was consistent through seasons. Yet, NCP was similar, and slightly negative, between the bare site and the oldest restored meadow on an annual basis, despite the vast differences in autotrophic biomass between the two sites (Rheuban et al., 2014a). Notably, summer metabolism revealed a net autotrophic state in the five-year-old meadow (NCP), whereas the older, mature meadow (11yr) had much higher metabolic fluxes and net heterotrophy on the order of about -50 mmol O_2 m^{-2} d^{-1} (Hume et al., 2011; Rheuban et al., 2014a).

Although GPP often substantially increases during summer in temperate seagrass meadows, so does CR to a similar extent (Ward et al., 2022). Consequently, despite large seasonal variability in photosynthesis and respiration, the metabolic state (NCP) is often relatively stable on an annual basis, granted there are no major ecosystem shifts. Interannual variability of NCP has been related to seagrass die-off and recovery episodes (Berger et al., 2020), and seagrass phenology typically dictate fluxes and metabolic state on intra-annual timescales (e.g. Champenois and Borges, 2012; Rheuban et al., 2014a). However, a seagrass meadow is comprised of several components that contribute to community metabolic fluxes. Aside from the seagrass itself, these include primary producers such as macro- and microalgae and heterotrophic organisms ranging from macrofauna to bacteria. Together, these make up the fluxes of O_2 and DIC measured in the overlying water column by methods such as aquatic eddy covariance, benthic chambers or open water mass balance. Isolating fluxes deriving from a single meadow component is difficult *in situ*, although promising efforts have been made at estimating the role of benthic fauna in meadow metabolism (Rodil et al., 2019; Rodil et al., 2020; Rodil et al., 2021; Rodil et al., 2022). When planting seagrass with the stated goals of obtaining both a carbon sink and a biodiversity hotspot, it is essential to understand the relationship between these two and over what timescales it may change as a meadow develops. It is therefore necessary to employ a holistic approach and assess biogeochemical and biodiversity parameters in tandem across multiple stages of seagrass growth. Importantly, both autotrophic and heterotrophic components of biodiversity are relevant as they are expected to have contrasting effects on metabolism.

The overarching goal of this study was thus to evaluate the alterations in metabolic fluxes and biodiversity across the transition from bare sediment to a mature seagrass meadow subsequent to active seagrass restoration. We hypothesized that in an early stage, autotrophic biomass is dominating but total biomass is relatively low, resulting in small diel variability in metabolic fluxes and an overall net autotrophic state. As the meadow grows, fauna colonization occurs alongside organic matter accumulation, shifting the system toward a more balanced metabolic state as |CR| increases relative to GPP. Finally, when the meadow has reached maturity, CR and GPP are tightly coupled in a system characterized by high turnover and a balanced NCP.

To test these hypotheses, we utilized a chronosequence of four stages of seagrass development since restoration located, all situated within the same sheltered bay. We employed non-invasive, high-resolution aquatic eddy covariance (EC) alongside benthic chamber incubations (BC). This allowed us to simultaneously monitor fluxes of O_2 and carbonate chemistry parameters from which we could evaluate daily metabolic fluxes of both

Deleted: all

Deleted: assess how

Deleted: change as the benthic environment evolves

Deleted: following

Deleted: es and

Deleted: builds up

Deleted: goes

Deleted: with

Deleted: in conjunction with

Deleted: From this we could

Deleted: record

oxygen and carbon. Additionally, we investigated multiple aspects of taxonomic and functional diversity among both macrophytes and benthic fauna and assessed surficial sediment carbon stocks to infer short-term impacts of seagrass restoration on both carbon cycling and biodiversity.

Deleted: features
Deleted: of
Deleted: effects

2. Methods

2.1 Site description

The study took place between July 4–20, 2022 on the island of Gåsö (58.2325, 11.3984) located at the mouth of the Gullmar fjord on the NW coast of Sweden (Fig. 1). The area has microtidal characteristics, with an amplitude of 20-30 cm, while the Gullmar fjord is stratified featuring three pycnoclines occurring between 10 – 50 m (Sundbäck et al., 2004). Surface water salinity naturally fluctuates between 15-30 in this region due to the alternating currents of brackish Baltic Sea water and saline North Sea water (Lindahl et al., 1998). The bay of Gåsö is a semi-enclosed bay spanning ~0.3 km^2 with two narrow inlets and outlets and lacks major surface freshwater sources. Its sheltered position results in a small fetch and a mild wave climate (Fig.1).

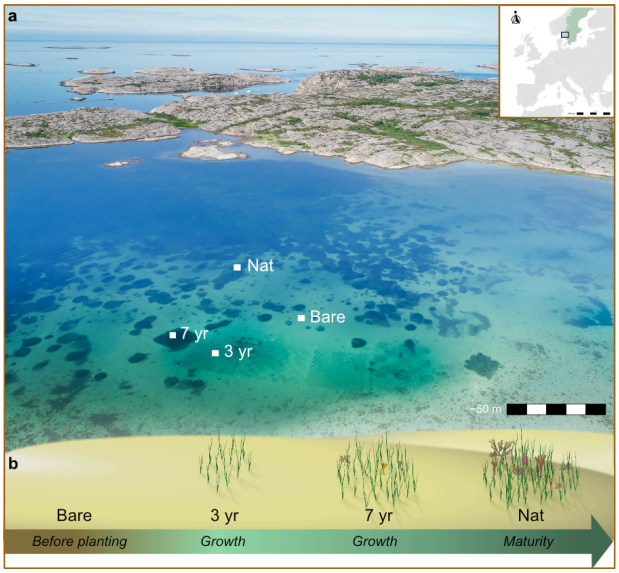

Figure 1 Aerial view and seagrass development stages after restoration. a) Map showing study location (inset) and drone image of Gåsö bay outlining the approximate locations of the sites, b) a schematic illustration of seagrass meadow development in the four sites Bare, 3 yr, 7 yr and Nat which represent different stages of meadow development as indicated by the arrow and text in italics.

The benthos consists of a natural, subtidal continuous eelgrass (*Z. marina*) meadow and large patches interspersed with bare sediment occurring between 1–4 m depth (Fig. 1; Huber et al., 2022). In 2015 and 2019, as part of the seagrass restoration program ZORRO (www.gu.se/en/research/zorro), two plots of *Z. marina* were planted at the same depth (~2 m), using the same planting methodology (single-shoot) and shoot density (16 shoots m^{-2}) (Gagnon et al., 2023). These plots thus provided a chronosequence of seagrass meadow ages spanning three and seven years since planting, while the bare sediment area and the natural meadow corresponded to a 'before' state and a mature meadow, respectively. The part of the natural meadow we sampled was estimated to have been naturally colonized by meadow expansion 13–15 years ago (E. Infantes, pers. obs.). Altogether, this yielded four sites within 100 m distance from each other representing four different stages in the development of a seagrass

Deleted: in

Deleted: west

Deleted: The bay of Gåsö is a semi-enclosed bay spanning ~0.3 km^2 with two narrow inlets and outlets.

Deleted: a)

Deleted: b)

Deleted: S

meadow (Fig. 1; Table S1). Importantly, the validity of applying a chronosequence methodology to investigate age-related differences in seagrass metabolism relies on assumptions that the sites compared experienced similar abiotic conditions after planting and during sampling (Fig. S2; Table S2). Utilizing adjacent sites within a semi-enclosed bay addresses most of those matters but to further control assumptions, we monitored *in situ* flow velocity, photosynthetic active radiation (PAR), temperature, turbidity, salinity and wind conditions during all deployments and assessed the variation in oxygen fluxes explained by each variable using linear mixed effects models (see below).

2.2 Benthic fluxes

2.2.1 Aquatic eddy covariance (EC)

The EC system (Berg et al., 2003) consisted of a stainless-steel tripod frame with an acoustic doppler velocimeter (ADV Vector, Nortek) and a fast-responding oxygen microsensor (430 UHS, Pyroscience GmbH) programmed to log data continuously at 16 Hz from co-located measurements of velocity and oxygen concentration. In addition, two PAR sensors (LI-192, RBR) were mounted to the frame where one was facing upwards to record incident light and one was directed downwards to record reflected light. This made it possible to calculate the fraction of absorbed light (*fAPAR*) during deployments. Dissolved oxygen optodes (miniDOT, PME and U26 HOBO, Onset) were mounted on the leg of the frame and recorded ambient dissolved oxygen concentration (DO) within the canopy at 1 min intervals. In addition, a salinity sensor (U24 HOBO, Onset), a turbidity sensor (RBRsolo, RBR) and two light intensity loggers (HOBO Pendant MX, Onset) were located on the frame recording at 1 min intervals.

We deployed the EC at the center of the transplanted plots, resulting in a distance of 20 m between the 3 yr and the 7 yr site. In order to maintain the same water depth, the bare site was located 46 m from the 7 yr and 29 m from the 3 yr site with the natural site 57 m away from the 3 yr site, 47 m from the 7 yr site and 58 m from the bare site (Table S1). EC deployments lasted between 44 and 49 hours (Table S1). In between each deployment data was offloaded, sensors and frame cleaned, and batteries exchanged as necessary.

2.2.2 Benthic chambers (BC)

Simultaneously with EC, we deployed benthic chambers (n=6 per site) within five meters of the EC and randomly emplaced within 1 m of each other (Fig. S1). We assured that chambers were positioned downstream of the EC with respect to the dominant current direction as to not influence the footprint of the EC. Benthic incubation chambers consisted of acrylic cylinders (inner diameter = 12.45 cm, length = 65 cm) with a custom-made motor running a propeller to mix the water within the chamber and avoid build-up of vertical concentration gradients. We employed pilot tests with dye injection in the laboratory and field to ensure sufficient mixing and during incubations, chambers were inserted approximately 20 cm into the sediment. We used transparent (n=3) and opaque (n=3) chambers to simulate day (photosynthesis and respiration) and night (respiration only), respectively. Upon deployment, chambers were left with lids off for about 30 mins to allow for suspended sediment to settle.

We drew discrete samples of seawater at onset and termination of each incubation using two 50 mL syringes attached to 30 cm Tygon® tubing, inserted through a closable sampling port in the chamber lid. We

immediately analyzed seawater in the syringes for pH and dissolved oxygen (DO). pH was measured using an InLab Micro pH electrode with a FiveGo handheld pH meter (Mettler Toledo). The electrode was calibrated both using a two-point calibration with standard buffers (pH 7 and 10, Mettler Toledo) at the onset and termination of the field campaign and calibrated to certified Tris buffer in synthetic seawater (Dr. A. Dickson, SIO) in the beginning and end of each sampling day. This was done to account for the effect of salinity and to yield values on the total hydrogen ion scale (pH_T). We measured salinity using a conductivity probe connected to a pH/cond 340i multimeter (WTW).

We measured DO using a fiberoptic oxygen sensor coupled to a FireSting® GO2 oxygen meter (PyroScience). A temperature probe was also connected to the FireSting® to record temperature during each measurement. Seawater from the syringes was then filtered through 0.45 µm Minisart® sterile syringe filters (Sartorius) and stored in 50 mL Falcon tubes on ice. Upon return to the laboratory, we placed samples for TA in a dark container at 4 ºC whereas samples for inorganic nutrients and DOC were frozen (-20 ºC) immediately until subsequent laboratory analyses.

We determined TA by open-cell potentiometric titration using an 888 Titrando system with an Ecotrode plus pH electrode (Metrohm). Samples (40–50 g) were titrated with prepared 0.05 M HCl in ~0.6 mol kg^{-1} NaCl, corresponding to the ionic strength obtained from the mean salinity of the samples. Accuracy and precision (-1.65±3.76 µmol kg^{-1}) were determined using certified reference material (CRM, batch 200, n=8) provided by Dr. Andrew Dickson at Scripps Institution of Oceanography, San Diego.

We analyzed dissolved inorganic nitrogen (NH_4-N and NO_3-N) using Flow Injection Analysis on a FIA Star 5000 analyzer (FOSS) and phosphate (PO_4-P) using ion chromatography on an 861 Advanced Compact IC (Metrohm). We analyzed dissolved organic carbon (DOC) and total nitrogen (TN) using a V-CPH Total Organic Carbon analyzer (Shimadzu).

We calculated DIC using the package *seacarb* in *R* (Gattuso et al., 2022) with measured values of pH_T and TA in conjunction with in situ temperature, salinity, pressure and NH_4^+ as input parameters. We used dissociation constants K_1^* and K_2^* from Lueker et al. (2000). We also calculated the saturation state of $CaCO_3$ mineral form aragonite ($\Omega_{Ar}=[Ca^{2+}][CO_3^{2-}]/K_{sp}^*$) from each sample using *seacarb*. All solute concentrations were calculated to µmol kg^{-1}, using *in situ* pressure, temperature and salinity data.

Using incubations with discrete measurements to assess flux rates assumes that concentrations change linearly with time. We verified this assumption *ex situ* by bringing an intact chamber core from the natural meadow into the laboratory. The chamber was placed in a large water bath with running seawater and prior to each incubation, the chamber was saturated with oxygen by bubbling compressed air. We ran multiple dark incubations with continuous logging of dissolved oxygen and temperature (FireSting® GO2) combined with multiple discrete measurements of pH (n=4) and TA (n=2).

We used the abovementioned measurements at the onset of incubations to infer mean ambient seawater chemistry at each site (Table S3).

Formatted: Font: Not Italic

2.3 Community components

2.3.1 Macrophytes and microphytobenthos

We evaluated seagrass shoot density by placing a 0.25 m x 0.25 m frame randomly in ten areas of each site and counting seagrass shoots in subareas of 0.016 m^2 (n=10 per site). In addition, we collected seagrass shoots using

a mesh net bag attached to a closable aluminum frame (opening area = 0.1156 m^2, n=3 per site). From these samples, we measured aboveground biomass, shoot density, number of reproductive shoots, leaf length, and number of leaves per shoot. We also assessed the taxa and biomass of macrophytes other than seagrass (e.g. red and brown macroalgae). Seagrass belowground biomass including live and dead roots and rhizomes were collected using sediment cores (see below). We dried biomass samples at 60 ºC for 72 hours and values are reported as dry mass (g m^{-2}).

We collected sediment samples to estimate microphytobenthos abundance, using sediment surface chlorophyll *a* as a proxy. From each sediment core, we used a cutoff 5-mL syringe (Ø=12 mm) to collect 2 mL sediment from the surface layer. This was repeated three times for each core and we pooled the three samples into one 6 mL sample per core and put in a 50 mL centrifuge tube covered in aluminum foil to avoid light penetration. The samples were immediately frozen (-20 ºC) until subsequent extraction and analysis. After thawing at 4 ºC overnight, we drew a subsample of 2 mL sediment from each sample, weighed and dried it at 60 ºC for 72 hours to obtain wet weight (g) dry weight (g), dry bulk density (DBD, g cm^{-3}) and water content (%). We extracted the chlorophyll using ethanol (99.5 %) and, after diluting and incubating overnight, measured fluorescence using a Turner TD-700 fluorometer (Turner Designs). We calculated chlorophyll *a* content (g m^{-2}) using a modified equation from Hannides et al. (2014).

Deleted:

Moved (insertion) [1]

Deleted: 2.3.4 Chlorophyll a¶

Formatted: Indent: First line: 1.27 cm

Deleted: for sediment surface chlorophyll *a* to serve as a proxy for

Formatted: Superscript

2.3.2 Benthic fauna

We targeted infauna and epifauna separately where we collected seagrass epifauna from the mesh net bag samples described above (mesh size ~ 0.2 mm, n=3 per site). This approach allows for capturing the entire community by which cores captures infauna and slow-moving epifauna and the mesh net approach captures fast-moving and larger epifauna present in the seagrass canopy. For infauna, we collected sediment cores using polycarbonate cylinders (inner diameter: 7.4 cm, length: 33 cm, 20 cm depth, n=6 per site) for determination of infauna and seagrass belowground biomass. Upon return to the laboratory, samples were sieved (0.5 mm) and fixed in 95 % ethanol for subsequent counting and species identification. Fauna was identified to lowest taxonomic level possible.

2.3.3 Sediment properties

In addition to the sediment cores used for infauna, we collected three additional sediment cores from each site to determine sediment properties. These cores were stored upright and immediately brought back to the lab and sliced into sections at 2, 4, 6, 8, 12, 16 cm depth. We used the top 0–2 cm section for determination of water content, DBD and porosity (refer to section 2.3.1). After removing all visible rhizomes, roots and shells, we dried all sections at 60 ºC for 72 hours, homogenized with a pestle and mortar and analyzed subsamples (5 mL) for organic matter content using loss on ignition (4 hours at 520 ºC). Subsamples from the top 0–2 cm sediment layer (n=12) were also analyzed for particulate organic carbon (POC), particulate inorganic carbon (PIC) and total nitrogen (TN) using a Vario MAX TN elemental analyzer (Elementar). We pre-treated samples with HCl to remove carbonates and PIC was obtained by subtracting POC from total carbon (TC). We obtained a linear relationship between OM and POC (POC=0.47*OM-0.88; R^2=0.84, $p<0.001$) which we used as a conversion factor to convert remaining OM values to POC and thereby obtain POC values for all core slices. This conversion is based on the assumption that the relationship persists with sediment depth and this introduces uncertainty in the

Deleted: chlorophyll *a*,

Deleted: dry bulk density (DBD, g cm^{-3})

Deleted: see below

Deleted: fragments

Deleted: remaining

Deleted: subsamples (5 mL)

POC values at depth. We calculated carbon density for each slice between 0–12 cm by multiplying POC with surface DBD and integrated across 0–12 cm to obtain the organic carbon stock (POC_{stock}, g m^{-2}) in the upper 12 cm of sediment. Using only DBD values for the top 0–2 cm introduces uncertainty in our depth-integrated POC_{stock} estimates but a previous study by Dahl et al. (2023) from the same area showed similar DBD values from 0–11 cm (mean 0.43±0.15 g cm^{-3}) that were consistent with sediment depth.

2.4 Data analyses

2.4.1 Flux calculations

We calculated oxygen fluxes in the benthic chambers (BC) as the difference in solute concentration between the onset and termination of each incubation as

$$F_{O2}\ (\text{mmol}\ O_2\ m^{-2}h^{-1}) = \frac{\Delta O_2}{\Delta t}\rho h \quad (1)$$

where ΔO_2 is the change in O_2 concentration in mmol kg^{-1} between start and end of incubation, dt is the duration of the incubation in hours, ρ is the density of the seawater in kg m^{-3} and h is the height of the chambers from the top to the sediment surface in meters. We calculated the flux of salinity-normalized TA (nTA = $TA/S_{in\ situ} \times S_{mean}$; Table S2) in the same way:

$$F_{TA}\ (\text{mmol TA}\ m^{-2}h^{-1}) = \frac{\Delta nTA}{\Delta t}\rho h \quad (2)$$

Similarly, we used DIC measurements to obtain fluxes as

$$F_{DIC}\ (\text{mmol C}\ m^{-2}h^{-1}) = \frac{\Delta nDIC}{\Delta t}\rho h - 0.5F_{TA} \quad (3)$$

where $\Delta nDIC$ is the change in salinity-normalized DIC in mmol kg^{-1}. The subtraction of $0.5F_{TA}$ is to account for the effect of inorganic processes (i.e. calcification/$CaCO_3$ dissolution) on DIC according to the assumptions that net community calcification affects TA and DIC in a ratio of 2:1 and NCP only modifies DIC (Smith and Key, 1975). F_{DIC} thus represents the DIC flux stemming from primary production and respiration only.

We calculated the photosynthetic (PQ) and respiratory (RQ) quotients from the average absolute fluxes (i.e. the magnitude of the flux, excluding the direction) in transparent and dark chambers, respectively, as

$$PQ = \frac{|F_{O2,light} - F_{O2,dark}|}{|F_{DIC,light} - F_{DIC,dark}|} \quad (4)$$

and

$$RQ = \frac{|F_{DIC,dark}|}{|F_{O2,dark}|} \quad (5)$$

Due to issues with the dark incubations in the natural meadow, RQ from this site was instead calculated as the average of the three other sites.

We computed EC fluxes from the high frequency time series following a multiple-step protocol described in Attard et al. (2019). In short, we bin-averaged the time series to 8 Hz, extracted fluxes for consecutive 15 min time windows using linear detrending (Mcginnis et al., 2014) and corrected fluxes for oxygen storage within the canopy (Rheuban et al., 2014b). Subsequently, we bin-averaged 15 min fluxes to 1 hr for interpretation. We defined F_{light} and F_{dark} based on when incident PAR was above or below 1 µmol m^{-2} s^{-1}, respectively. All sites experienced 19 light hours and 5 dark hours on average. We calculated daily metabolic parameters gross primary productivity (GPP) as

Moved up [1]: 2.3.4 Chlorophyll a
We collected samples for sediment surface chlorophyll *a* to serve as a proxy for microphytobenthos. From each sediment core, we used a cutoff 5-mL syringe (Ø=12 mm) to collect 2 mL sediment from the surface layer. This was repeated three times for each core and we pooled the three samples into one 6 mL sample per core and put in a 50 mL centrifuge tube covered in aluminum foil to avoid light penetration. The samples were immediately frozen (-20 ºC) until subsequent extraction and analysis. After thawing at 4 ºC overnight, we drew a subsample of 2 mL sediment from each sample, weighed and dried it at 60 ºC for 72 hours to obtain wet weight (g) dry weight (g), DBD and water content (%). We extracted the chlorophyll using ethanol (99.5 %) and, after diluting and incubating overnight, measured fluorescence using a Turner TD-700 fluorometer (Turner Designs). We calculated chlorophyll *a* content (g m^{-2}) using a modified equation from Hannides et al. (2014).

$$GPP\ (\text{mmol}\ m^{-2}d^{-1}) = \left(F_{light} + |F_{dark}|\right) \times t_{day} \quad (6)$$

where t_{day} is the number light hours. We calculated community respiration (CR) as

$$CR(\text{mmol}\ m^{-2}d^{-1}) = F_{dark} \times 24 \quad (7)$$

and net community productivity (NCP) as

$$NCP\ (\text{mmol}\ m^{-2}d^{-1}) = GPP - |CR| \quad (8)$$

We converted oxygen-based daily metabolic fluxes to DIC fluxes by multiplying F_{light} and F_{dark} with our empirically derived PQ and RQ, respectively:

$$F_{light\_DIC}\ (\text{mmol DIC}\ m^{-2}h^{-1}) = F_{light} \times \frac{1}{PQ} \quad (9)$$

$$F_{dark\_DIC}\ (\text{mmol DIC}\ m^{-2}h^{-1}) = F_{dark} \times -\overline{RQ} \quad (10)$$

We then recalculated daily metabolic DIC fluxes GPP_{DIC}, CR_{DIC} and NCP_{DIC} (mmol DIC m^{-2} d^{-1}) using Eq. (6) – (8). Due to lack of information on the temporal variability in PQ and RQ, we only interpret DIC fluxes on a daily basis.

2.4.2 Biodiversity

We evaluated biodiversity both from a taxonomic and a functional perspective. For taxonomic diversity, we used the *vegan* package in R (Oksanen et al., 2019) to compute Shannon diversity (H') and Pielou's evenness component (J'). H' was converted to effective numbers (H_{eff}=exp(H')) to make it linear and scale to species richness (Jost, 2006). For functional diversity, we first assigned functional traits to each species based on existing literature (Österling and Pihl, 2001; Törnroos and Bonsdorff, 2012; Queirós et al., 2013; Riera et al., 2020; Remy et al., 2021; Kindeberg et al., 2022) and the databases Biological Traits Information Catalogue (Marlin, 2023) and Polytraits (Faulwetter et al., 2014). The selection of functional traits was based on direct connections to carbon cycling including feeding mode, bioturbation mode and whether the species is calcifying. Indirect, general traits included movement mode, living habit and environmental position. This selection process resulted in 25 trait modalities from which we constructed a traits-by-species matrix assigning each species to specific trait modalities (refer to Table S4). Species can exhibit multiple trait modalities, depending on life history and environmental conditions. To address this, and to avoid a disproportionally large influence by generalist species on functional diversity, we used fuzzy coding (Chevenet et al., 1994) whereby species comprising multiple trait modalities were assigned a score between 0 (no association) and 3 (full association), with the total sum of each trait always being 3. Based on this matrix, we calculated community-weighted means of trait values (CWM) and several multivariate components of functional diversity including functional richness (FRic), functional evenness (FEve) and Rao's quadratic entropy (RaoQ). These calculations were performed using the *FD* package in R (Laliberté and Legendre, 2010) and further detailed information on these multivariate components and their taxonomic analogs can be found in Mason et al. (2005) and Villéger et al. (2008). As with H', the functional diversity index RaoQ was transformed to effective numbers as FD_{eff} = 1/(1-RaoQ).

We measured biomass divided into classes. We obtained wet weight (g) after blotting each specimen on a tissue for two seconds and dry weight (g) after drying at 60 °C for 24 hours. Regrettably, due to a computer malfunction the class division per sample was lost for infauna samples and only total, pooled biomass per site is

Deleted: We then
Deleted: categories
Deleted: 3
Deleted: (Gbenebor et al., 2016)
Deleted: categories

available for this group. We combusted pooled samples at 520 °C for 4 hours to obtain ash-free dry weight (AFDW, g m^{-2}).

2.4.3 Light-use efficiency

We evaluated the relationship between irradiance (PAR) and gross primary productivity (GPP) using a hyperbolic tangent function (Jassby and Platt, 1976; Platt et al., 1980):

$$GPP = P_m \times \tanh\left(\frac{\alpha PAR}{P_m}\right) \quad (11)$$

where P_m is maximum oxygen flux of gross primary productivity (mmol O_2 m^{-2} h^{-1}), α is the quasi-linear initial slope of the curve and PAR is seabed irradiance as photosynthetic active radiation (µmol photons m^{-2} s^{-1}). We performed curve-fitting in OriginPro 2022 using a Levenberg–Marquardt iteration algorithm, and we scaled the standard error of the fitting parameters with the square root of the reduced chi squared statistic (Attard & Glud 2020).

To examine these relationships further, we calculated the light-use efficiency (LUE) at each site, which indicates the efficiency with which absorbed PAR is converted to primary production, as:

$$LUE = \frac{GPP}{PAR \times fAPAR} \quad (12)$$

where fAPAR is the fraction of absorbed irradiance calculated from the difference between incident and reflected PAR as measured by the upward and downward facing PAR sensors (see above). Including fAPAR in the calculation of LUE thereby accounts for any differences owing to meadow characteristics such as the higher three-dimensional meadow complexity (higher fAPAR) relative to bare sediment (lower fAPAR) and captures the diel differences in seabed reflectance and absorption (Attard and Glud, 2020).

2.4.4 Statistical models

To test the effect of differences in abiotic factors between deployments, and thereby validate the use of the chronosequence approach, we employed linear mixed-effects models (package *lme4* in R (Bates et al., 2015), testing the effect and interaction of abiotic variables on absolute values of hourly oxygen fluxes ($|F_{O2}|$). We used model selection (based on Akaike information criterion, AIC) to select the best model, which included sea surface temperature, flow velocity, PAR and turbidity as fixed effects and site as a random factor. We used type III ANOVA for significance testing of fixed effects and likelihood-ratio tests (LRT) for the random effect. Assumptions of models were tested using the *performance* package in R (Lüdecke et al., 2020). We assessed differences in oxygen fluxes calculated by the EC and BC using a two-sample t-test and compared oxygen and DIC fluxes in the benthic chambers using linear regression analyses. We tested site differences in biodiversity and sediment parameters using multiple one-way ANOVAs and visually reviewed multivariate community composition using non-metric multidimensional scaling (NMDS) and principal components analyses (PCA). We set significance level to α=0.05 for all statistical tests and performed all analyses in R, version 4.2.3 (Rcoreteam, 2023).

Deleted: and

Deleted: o

2.4.5 Carbon budget

We constructed a carbon budget of daily inorganic carbon fluxes and pools of organic carbon. We based the sediment carbon pool on the POC stock of the top 12 cm of sediment whereas we inferred seagrass aboveground

and belowground carbon from dry weight (DW) and a global average carbon content for *Z. marina* of 34 % DW (Duarte, 1990). We estimated macroalgal carbon content based on DW and species-specific carbon content of the dominant red and brown algae reported from the area, which ranged from 29.1–39.9 % DW (Olsson et al., 2020). For benthic fauna, we converted ash-free dry weight (AFDW) to carbon, assuming a 50 % carbon content (Wijsman et al., 1999; Rodil et al., 2021). We converted organic carbon pools to moles and they are reported as mol C m^{-2}. Lastly, we calculated the total pool of organic carbon for each site as the sum of all pool means. We calculated the total propagated uncertainty (SE_{total}) as:

$$\boldsymbol{SE_{total}} = \sqrt{\sigma^2_{sediment} + \sigma^2_{AG} + \sigma^2_{BG} + \sigma^2_{algae} + \sigma^2_{fauna}} \Big/ \sqrt{\boldsymbol{n}} \quad (13)$$

where σ is the standard deviation of each pool mean and n is the number of pools. AG and BG is eelgrass aboveground and belowground biomass, respectively.

3. Results

3.1 Environmental conditions

The weather was sunny and dry during all field deployments with only two minor rain events in between (Fig. S2). Sea surface temperature ranged from 17.10–19.98 ºC, driven mainly by the diel light cycle. Salinity ranged from 24.7 to 28.9 but remained constant (±0.1) during each individual deployment. Photosynthetic active radiation (PAR) at the seabed was similar between sites and deployments and reached a highest value of 728 µmol m^{-2} s^{-1} (Fig. 2; Fig. S2). Flow velocities ranged from 0.9 to 21 cm s^{-1}, averaging 5.6±3.4 cm s^{-1} across all sites (Fig. 2; Fig. S2).

Ambient seawater chemistry was largely similar between sites, although there was a higher background salinity, TA, DIC and DIN at the 3 yr and Nat site, which were sampled after a weather front passed by likely exchanging some of the bay water with off-shore fjord water (Table S3; Fig. S2). Average DO during EC deployments was highest in Bare and lowest in 3 yr, averaging (mean±sd) 302.9±21.8 and 260±37.3 µM, respectively. Turbidity was generally low but increased markedly at the Nat site, following a minor rain event prior to deployment (Fig. S2; Table S2). Yet, differences in turbidity did not have any detectable effects on seabed PAR (Fig. S2; Table S2).

3.2 Hourly oxygen fluxes

Hourly O_2 fluxes followed the diel light cycle and increased both in magnitude and variability going from bare sediments to increasing age of the restored seagrass (Fig. 2).

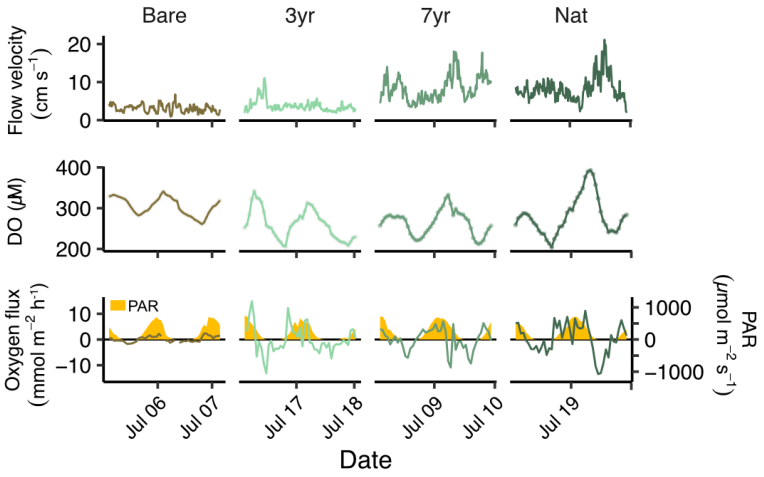

Figure 2 Time series of flow, oxygen and light. Time series of (a) flow velocity, (b) ambient dissolved oxygen and (c) hourly oxygen flux overlaid on photosynthetic active radiation (PAR) in yellow.

The largest hourly oxygen fluxes typically occurred in the afternoon, with highest recorded between 14:30–15:30 in the 3 yr site (8.96±1.44 mmol m^{-2} hr^{-1}). The largest oxygen uptake rates were generally observed during hours following midnight, with the most negative hourly flux recorded between 23:30–00:30 in Nat (-9.08±5.62 mmol m^{-2} hr^{-1}).

Deleted: 1
Deleted:
Deleted: 1
Deleted: 1
Deleted: 1
Deleted: 1

Flow velocity was on average significantly higher in the 3 yr compared to Bare and significantly higher in the 7 yr and Nat meadow compared to the 3 yr (Table S2). Although there was a general positive linear relationship between flow velocity and absolute oxygen flux across all deployments, the higher flow velocities in 7 yr and Nat generally occurred during short time periods at night and did not correspond to consistent increases in absolute oxygen fluxes for those sites (Fig. S3). Consequently, site R^2 values were low ranging from <0.001 – 0.20 (Fig. S3). Further analysis through linear mixed effects modelling indicated that while temperature, PAR, turbidity and flow velocity explained 20% of the variation in hourly $|F_{O2}|$ across all sites, the random effect Site was highly significant (LRT = 20.9, $p < 0.001$) suggesting that some other feature, not included in the model, contributed to the observed differences in oxygen fluxes between sites (Table S5).

3.3 Daily integrated metabolism

Daily metabolic oxygen fluxes (GPP, CR) as measured by the EC were lowest in the bare sediments and increased with meadow age (Fig. 3a). GPP and CR were tightly coupled but |CR| was always higher than GPP, amounting to an average GPP:CR ratio of 0.81 (Fig. 3b). Accordingly, we observed net heterotrophy at all sites (NCP < 0; Fig. 3a–b). Oxygen-based NCP decreased three-fold between the bare and the youngest restored meadow (-5 to -15 mmol m^{-2} d^{-1}) with a further 40 percent decrease in the seven-year-old meadow (-21 mmol m^{-2} d^{-1}).

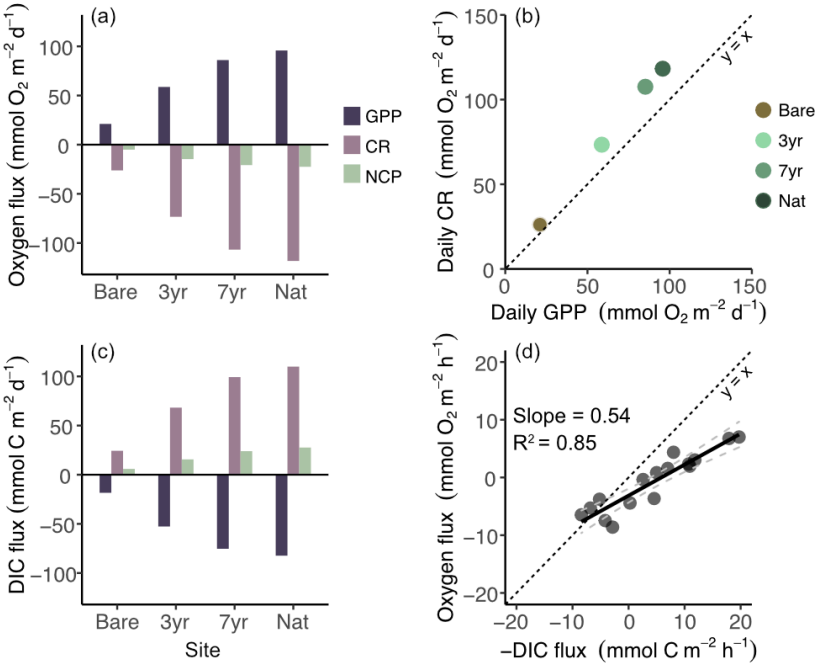

Figure 3 Fluxes and relationships of oxygen, carbon and productivity dynamics. a) Daily oxygen fluxes as gross primary productivity (GPP), community respiration (CR) and net community productivity (NCP). b) Linear regression of daily oxygen-based GPP and CR; c) Daily dissolved inorganic carbon (DIC) fluxes based on eddy covariance fluxes converted using photosynthetic (PQ) and respiratory (RQ) quotients d) Linear regression of oxygen and dissolved inorganic carbon (DIC) hourly flux measured in the benthic chambers used to calculate PQ and RQ. Dashed black line indicates slope=1 and dashed grey lines are 95 % confidence interval of the fitted slope.

Oxygen fluxes measured by the EC and BC were not significantly different from each other (two-sample t test: $p = 0.69$), although there was a tendency to overestimate oxygen fluxes in BC relative to EC by 0.7–4.0 mmol m^{-2} hr^{-1}. Oxygen and DIC fluxes in the benthic chambers were highly correlated across all incubations (Fig. 3d), irrespective of differences in light conditions. The photosynthetic quotient (PQ) was always less than unity, averaging 0.46±0.10 across the four sites, whereas the respiratory quotient (RQ) averaged 0.93±0.25. Site-specific RQ revealed high variability between sites ranging from 0.65–1.13.

Estimated DIC fluxes mirrored those of O_2 and the benthic DIC net efflux (NCP_{DIC}) increased as a function of meadow age from 6 mmol m^{-2} d^{-1} in the bare sediments to 28 mmol m^{-2} d^{-1} in the natural meadow, thus confirming the net heterotrophic status of the meadows as determined using oxygen fluxes (Fig. 3b, 3c).

3.4 Structural and functional diversity

3.4.1 Meadow properties

All three eelgrass sites were characterized by high spatial heterogeneity within each meadow (Table 1). No significant differences were observed in seagrass morphometry such as shoot density, canopy height or below- or aboveground biomass. The only seagrass parameter that differed between the meadows was the number of reproductive shoots containing seeds, which was significantly higher in the natural meadow ($p = 0.004$). However, the abundance and biomass of other macrophyte species such as brown and red macroalgae increased markedly with meadow age. In the 3 yr meadow, only a small specimen of the brown algae *Spermatochnus paradoxus* was found in one sample whereas in the natural meadow large quantities of up to five different macroalgal species were found. However, due to large variability in biomass between samples within each site (Table 1), the between-site differences in number of species were not statistically significant (ANOVA, $p>0.05$). The composition of macrophyte species became more even with meadow age such that while the 3 yr meadow was dominated by *Z. marina* (~99 % of total macrophyte biomass), the 7 yr and the natural meadow had a more heterogenous and evenly distributed macrophyte community, where *Z. marina* on average contributed 90±15 % and 64±32 %, respectively, to total macrophyte biomass (Table 1). As a result, the three-dimensional complexity of the canopy increased with meadow age, driven mainly by large-bodied drifting fucoid species (*F. serratus* and *F. vesiculosus*) and red algae *Furcellaria lumbricalis* residing, unattached, within the canopies.

Benthic microalgae, as inferred from chlorophyll *a* on the sediment surface, showed the opposite trend and decreased with meadow age and chlorophyll *a* was significantly lower in sediments underlying 7 yr (0.28±0.03 g m^{-2}) and Nat (0.26±0.01 g m^{-2}) compared to Bare (0.56±0.07 g m^{-2}).

Table 1 Eelgrass and macroalgal structural diversity. Morphometrics, biomass and diversity across the sites (mean±SE). 'Rep. shoots' represents reproductive shoots with seed spathes present. AG and BG are aboveground and belowground eelgrass biomass, respectively, as captured by sediment cores. Macroalgal biomass represents macroalgae collected from eelgrass canopy samples. Maximum number of species refers to the count of macroalgal species found in a sample. Relative proportion indicates macroalgal biomass relative to total macrophyte biomass. Species richness, diversity (H_{eff}) and evenness (J') refer to macrophytes including macroalgae and eelgrass. An asterisk indicates statistical significance ($p<0.05$).

Parameter	Unit	3 yr	7 yr	Nat
		Eelgrass		
Shoot density	m^{-2}	153±21	153±14	151±21
Shoot length	cm	43.3±2.1	39.0±0.2	40.0±1.2
Rep. shoots	m^{-2}	9±5	3±3	32±3*
AG biomass	g m^{-2}	190.4±38.4	121.4±17.7	151.6±52.0

Deleted: within and

Deleted: We did not observe any

Deleted: that were

Deleted: of

Deleted: in

Deleted: and m

Deleted: number

Deleted: is the

Formatted: Superscript

AG core	g m^{-2}	117.3±77.8	132.5±67.0	108.9±49.2
BG core	g m^{-2}	126.4±63.3	259.6±54.7	104.3±59.4
AG:BG	-	2.6±1.6	0.5±0.2	0.8±0.2
		Macroalgae		
Macroalgal biomass	g m^{-2}	0.004±0.004	16.3±15.4	131.6±94.3
Max no. of species	-	1	2	4
		Macrophyte diversity		
Relative proportion	%	0.002±0.002	9.4±8.7	35.6±18.4
Species richness		1.3±0.3	3±0	3.3±1.5
Diversity (H_{eff})	-	1.0±0.0	1.3±0.3	2.1±0.6
Evenness (J')	-	0.001±0.0	0.2±0.2	0.7±0.0

3.4.2 Benthic fauna

We collected a total of 1927 individuals representing 43 taxa. Taxonomic diversity parameters (abundance, number of species, Shannon diversity, evenness) exhibited large within-site variability, highlighting the small scale (<10 m) heterogeneity of fauna community structure. These parameters consistently showed higher values in vegetated compared to bare sediments but exhibited variable, but generally non-significant, differences between the eelgrass sites (Fig. 4; Table S6). Abundance of infauna was highest in the 3 yr site, primarily dominated by opportunistic polychaetes (e.g. *Capitella capitata*). Yet, despite the high abundance in the 3 yr site, this site did not show a corresponding spike in infaunal species richness but was reflected by the lowest evenness among all sites (J'=0.47±0.08). By contrast, in the 7 yr, the abundance had decreased by a third while species diversity (H_{eff}) and evenness (J') nearly doubled, exhibiting similar values as the natural reference meadow (Table S6). Functional trait metrics revealed that both the functional group richness (FGR) and functional diversity (FD_{eff}) were significantly higher in the 7 yr and Nat compared to the 3 yr and Bare sites which exhibited similar values (Table S6). Functional richness (FRic) was notably low in the bare sediments (0.06±0.05) and tended to increase with meadow age peaking with the highest mean value in the natural meadow (0.53±0.11). However, due to high within-site variability, FRic did not show statistically differences between sites (Fig. 4c).

When separately targeting the meadows for epifauna, we found that they were species rich and highly diverse, ranging from 15–18 species and H_{eff} from 7.4–10.9. However, neither taxonomic nor functional diversity metrics exhibited any significant differences between the meadows, although there were some increasing trends particularly in functional evenness (FEve), which was highest in Nat and lowest in 3 yr (Table S6). Epifaunal biomass increased on average three-fold in Nat compared to the two restored meadows, displaying the highest within-site variability (15.89±10.48 g m^{-2}), primarily driven by gastropods.

Community composition partly shifted as the meadow grew whereby bare sediments and the youngest restored meadow were dominated by polychaetes whereas more epifaunal species such as bivalves and crustaceans were found in older meadows (Fig. 4d). Absolute abundances and biomass supported these observations, with bryozoans and gastropods contributing to higher biomass in Nat relative to Bare. However, multivariate analysis of the different communities indicated an overlap in community composition (Fig. S4).

Our analysis of functional traits highlighted the prevalence of certain bioturbation modes in relation to meadow age. For instance, community-weighted means (CWM) of biodiffusors displayed a linear increase with meadow age and was significantly higher in the natural meadow and 7 yr compared to the 3 yr ($F_{3,20}$ = 8.4; p <

Deleted: belonging to
Deleted: illustrating
Deleted: were always
Deleted: relative
Deleted: 2
Deleted: result
Deleted: in
Deleted: total
Deleted: biomass
Deleted: of
Deleted: l
Deleted: 2
Deleted: was
Deleted: 2
Deleted: obtaining
Deleted: but
Deleted: was
Deleted: t
Deleted: in especially
Deleted: 2
Deleted: and also had
Deleted: mainly
Deleted: increased
Deleted: this
Deleted: of which also
Deleted: ed
Deleted: visualization
Deleted: that there was much
Deleted: 3
Deleted: Based on our functional
Deleted: analyses,
Deleted: became more prevalent as a function of
Deleted: (Table S3).
Deleted: increased
Deleted: ly

0.001). Surficial modifiers among infauna were higher in eelgrass compared to bare sediment, peaking in the oldest restored meadow at a CWM of 0.29±0.10.

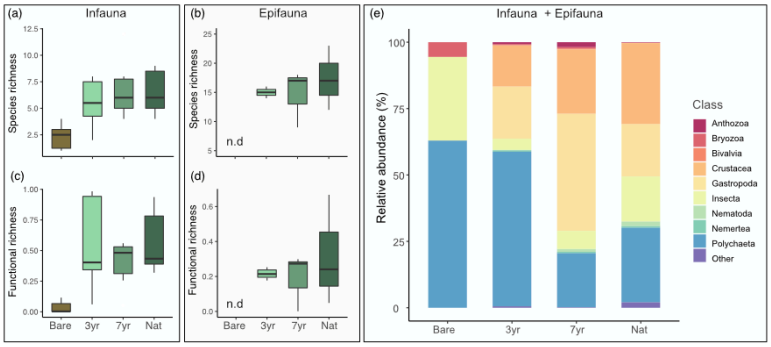

Figure 4 Biodiversity patterns in benthic fauna. Panels to the left show species richness (a–b) and functional richness (c–d) of infauna samples (a & c) and epifauna samples (b & d). Large panel to the right (e) shows relative abundance of different classes of all fauna combined (infauna + epifauna).

3.5 Sediment carbon stocks

The sediment within Gåsö bay eelgrass meadows has previously been reported as silty sand, with a median grain size (D_{50}) of the surface sediment between 140–170 µm and a silt-clay content of 26-35% (Infantes et al., 2022; Dr. Martin Dahl, pers. comm.). Concentrations of sediment OM, POC and TN were not significantly different between sites ($p < 0.05$) and did not display any consistent increases or decreases with meadow age (Table 2). However, when integrating the POC density across the top 12 cm, the highest POC stock was found in one natural meadow core (1529 g m^{-2}) and the lowest in a bare sediment core (209 g m^{-2}). Yet, due to large within-site variability, the sites were not significantly different from each other ($F_{3,8}$=1.52; p=0.28; Table 2). Meadow age did not show a clear trend, as demonstrated by the 3 yr site, which had an average carbon stock 32 % larger than the 7 yr, while the 7 yr site was more similar to the bare sediments site (Table 2). Depth profiles of POC concentration and density down to 20 cm revealed near-constant values down to between 12–16 cm, where increase was observed (Fig. S5). Natural eelgrass had the highest average POC profile, but average values were highly skewed by one core replicate displaying POC density four times higher than the other two replicates within the site.

Table 2 Sediment properties across sites. Organic matter (OM), particulate organic carbon (POC), particulate inorganic carbon (PIC), total nitrogen (TN) and dry bulk density (DBD) of the top 2 cm of sediment. POC stock is the depth-integrated carbon stock over 0–12 cm sediment depth. Values are mean±SE, n=3 per site.

Site	OM (%)	POC (%)	PIC (%)	TN (%)	DBD (g cm^{-3})	POC_{stock} (g m^{-2})
Bare	3.80±0.23	0.88±0.14	0.55±0.06	0.25±0.02	0.37±0.08	343±93
3 yr	5.42±0.56	1.76±0.26	0.18±0.04	0.34±0.03	0.37±0.07	652±142
7 yr	5.36±0.34	1.54±0.31	0.61±0.21	0.34±0.01	0.24±0.03	494±39
Nat	4.98±0.78	1.11±0.11	0.64±0.30	0.29±0.04	0.34±0.06	883±332

Deleted: and
Deleted: ed
Deleted: a
Deleted: The lack of
Deleted: with meadow age was further
Deleted: , on
Deleted: ,
Deleted: carbon stock
Deleted: and
Deleted: in turn
Deleted: it started to
Deleted: 4
Deleted: as
Deleted: as

3.6 Light-use efficiency

All meadows experienced similar incident light conditions (Fig. 5a). The fraction of absorbed light (*f*APAR) was always higher in eelgrass (~97 %) compared to bare sediments (~94 %) but did not differ between eelgrass sites on a daily basis (Fig. 5b). Hourly GPP tracked PAR with a clear hysteresis effect evident in the 7 yr and natural meadow but to a lesser extent in the bare site (Fig. 5c; Fig. S6). P-I relationships were best explained by the hyperbolic tangent function yielding R^2 between 0.45–0.74. The irradiance needed for photosynthesis to balance respiration (I_k) was almost four times higher in the bare site compared to the 7 yr site, equaling 380 and 97 µmol photons m^{-2} s^{-1}, respectively (Table S7; Fig. 5d). Estimated light-use efficiency (LUE) was lowest in Bare (0.001 O_2 $photon^{-1}$) and increased with meadow age to 0.004 and 0.005 O_2 $photon^{-1}$ in 3 yr and 7 yr, respectively. The highest daily LUE was observed in Nat (0.007 O_2 $photon^{-1}$) coincident with the highest number of macrophyte species and the most diverse community structure (Fig. 6).

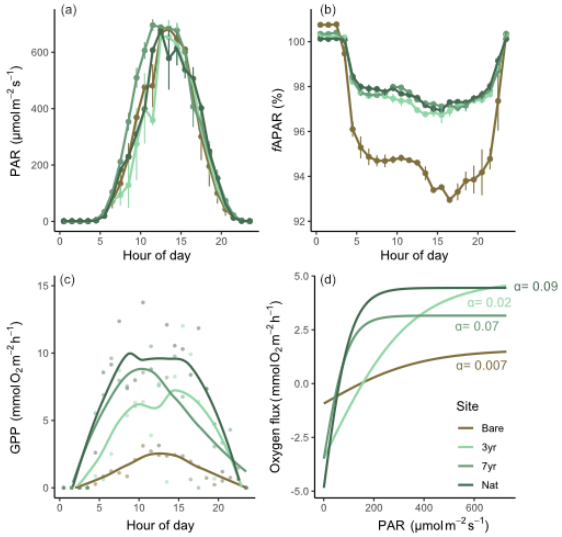

Figure 5 Light-use efficiency and productivity relationships. Panels a–c show different components of light-use efficiency (LUE) as a function of hour of the day: a) incident photosynthetic active radiation (PAR); b) fraction of absorbed PAR (fAPAR); c) shows gross primary productivity (GPP) as a function of time of day and; d) shows the relationship between oxygen flux and PAR as hyperbolic tangent curves estimated for each site.

Similar to LUE, GPP and |CR| displayed a positive linear relationship with number of macrophyte species. There was also a positive trend between these parameters and macrophyte Shannon diversity (H_{eff}) and the proportion of macroalgal biomass relative to eelgrass biomass, respectively (Fig. 6). As such, the model that best explained changes in daily benthic metabolism across the four different stages of seagrass development was a logarithmic model (Table 3).

Table 3 Daily metabolism as a function of meadow age. Curve fitting of daily metabolism parameters GPP, CR and NCP to meadow age (SiteAge) converted to logarithmic scale ($log_{10}(x+1)$). SiteAge for the site Bare was defined as 0 and 13 years for the natural meadow.

Metabolic parameter	Function	p	R^2

Deleted: 5

Deleted: 4

GPP	$GPP = 67.29 \pm 4.63 \times \log_{10}(\text{SiteAge} + 1) - 20.80 \pm 3.65$	0.005	0.99
CR	$CR = -83.08 \pm 5.77 \times \log_{10}(\text{SiteAge} + 1) - 26.06 \pm 4.56$	0.005	0.99
NCP	$NCP = -15.79 \pm 1.26 \times \log_{10}(\text{SiteAge} + 1) - 5.26 \pm 0.99$	0.006	0.98

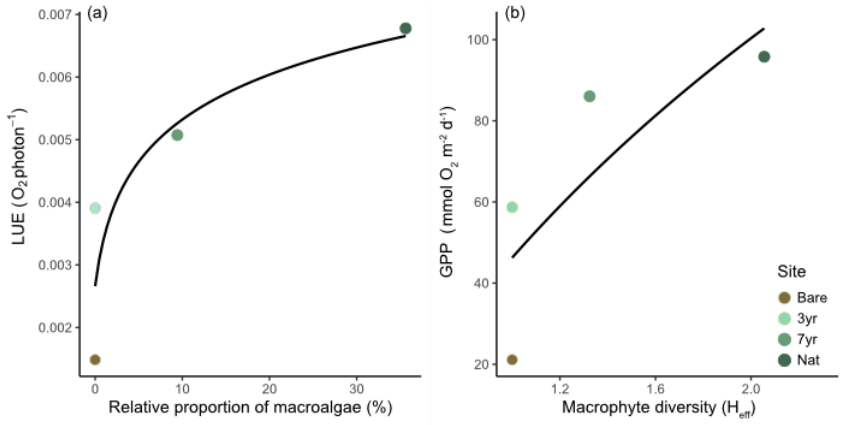

Figure 6 Biodiversity and productivity relationship. (a) Light-use efficiency (LUE) as a function of the relative biomass of macroalgae to eelgrass ($R2_{adj}$= 0.70). (b) Gross primary productivity (GPP) as a function of macrophyte Shannon diversity index ($R2_{adj}$= 0.46); Black lines represent best fit ($\log_e(x+1)$). Note that the bare site was not quantitatively sampled for macroalgal proportions or macrophyte diversity and was *a posteriori* set to 0 % and 1, respectively, for curve fitting.

Formatted: Font: Italic

Deleted: in

3.7 Carbon pools

Converting seagrass community components to carbon illustrates the pools of carbon available for export, remineralization or burial. Notably, total carbon pools were higher in eelgrass relative to bare sediment but were similar between restored and natural seagrass (Table 4). Sediment POC stocks were the largest carbon pools followed by eelgrass biomass which contributed on average 11, 21 and 7 percent to the total carbon pool in the 3 yr, 7 yr and natural meadow, respectively (Table 4).

Table 4. Carbon pools. Pools of particulate organic carbon (mean±SE, mol C m^{-2}) in the different components of the benthic habitats. AG and BG are above- and belowground eelgrass biomass, respectively. Fauna is total fauna (infauna+epifauna).

Site	Sediment	Eelgrass AG	Eelgrass BG	Macroalgae	Fauna	Total pool
Bare	28.54±7.71	0	0	n.d.	0.03	28.57±13.35
3yr	54.28±11.83	3.32±2.20	3.58±1.79	0.00±0.00	0.24	61.42±10.82
7yr	41.15±3.27	3.75±1.90	7.35±1.55	0.45±0.42	0.29	52.99±4.14
Nat	73.53±27.65	3.08±1.39	2.95±0.69	3.78±2.76	0.56	83.91±24.14

4. Discussion

We present a comprehensive dataset documenting post-restoration seagrass development that captures several aspects of seagrass metabolism. This dataset enables investigating the role of biodiversity and different components of a seagrass ecosystem in carbon cycling. We show that i) community-integrated photosynthetic (GPP) and respiratory (CR) fluxes increase as a function of meadow age (Fig. 3); ii) daily |CR| increased more relative to GPP resulting in net heterotrophy (NCP<0) on diel timescales during summer; iii) diversity and biomass of macrophytes other than the restored seagrass could be driving higher primary productivity through increased light-use efficiency (Fig. 5); iv) faunal communities recover rapidly and attain species- and functional richness comparable to natural meadows within seven years since restoration (Fig. 4); v) surficial (0–12 cm) sediment carbon stocks are large but are not significantly affected by the presence of seagrass in this sheltered bay.

Based on the above results, we postulate that while increased macrophyte diversity enhances both GPP and CR, the additional CR stemming from benthic fauna communities together with labile organic matter input push diverse seagrass meadows toward net heterotrophy during summer. This highlights potential tradeoffs between climate change mitigation and biodiversity conservation as incentives for seagrass restoration. Below we discuss four primary lines of evidence to support this postulation.

4.1 Metabolic fluxes scale to meadow development

We found large daily fluxes of GPP- and CR derived O_2 and DIC that increased as the system developed from bare sediments to a mature meadow (Table 3; Fig. 3). Our values (mean±SE) of GPP, CR and NCP across the three seagrass sites were 80±11, -99±13 and -19±2 mmol O_2 m^{-2} d^{-1}, respectively, which is relatively low when comparing to global average GPP, CR and NCP estimated for temperate seagrasses of 166±14, -130±11 and 34±8 mmol O_2 m^{-2} d^{-1}, respectively (Duarte et al., 2010). Yet, it should be noted that discrepancies owing to methodological differences are difficult to account for. An updated assessment of seagrass NCP in temperate areas reported an average of 29±79 mmol O_2 m^{-2} d^{-1}, although the study which covered 187 seagrass metabolism studies found that merely 68 % reported net autotrophy (Ward et al., 2022). Accordingly, the notion that seagrass habitats are strongly net autotrophic is being increasingly contested as methods continue to improve. In all our sampled sites, GPP was lower than |CR| resulting in net heterotrophy (negative NCP), independently established both by EC oxygen fluxes and benthic chamber DIC and oxygen fluxes. Several recent studies have reported instances of sustained net heterotrophy across multiple seagrass species and environments (e.g. Barron et al., 2006; Rheuban et al., 2014a,b; van Dam et al., 2019; Berger et al., 2020; Attard et al., 2019; Berg et al., 2022, Ward et al., 2022). For instance, a recent study of *Z. marina* using EC reported GPP and CR values similar to our natural meadow (95 and 94 mmol O_2 m^{-2} d^{-1}, respectively) resulting in a near balanced metabolic state across 11 years of monitoring (Berger et al., 2020). The authors reported a generally balanced metabolic state on monthly timescales but following a temperature-driven dieback event that diminished seagrass shoot density, GPP and |CR| decreased by 55 % and 48 %, respectively. This shifted the meadow to net heterotrophy during summer (NCP = -26±15 mmol O_2 m^{-2} d^{-1}). In the following years, the gradual increase in seagrass shoot density increased primarily GPP, showing clear signs of seagrass recovery (Berger et al., 2020).

Although GPP often substantially increases during summer in temperate seagrass meadows, so does CR to a similar extent (Ward et al., 2022). Consequently, despite large seasonal variability in photosynthesis and

Deleted: of
Deleted: different components
Deleted: higher
Deleted: of macrophytes contribute to elevated
Deleted: summer
Deleted: illustrates
Deleted: main
Deleted: values
Formatted: Subscript
Formatted: Superscript
Formatted: Superscript
Deleted: are

respiration, the metabolic state is often relatively stable on an annual basis, granted there are no major ecosystem regime shifts. While interannual variability of NCP has been related to seagrass die-off and recovery episodes (Berger et al., 2020), seagrass phenology linked to abiotic factors such as temperature and light regimes typically dictates the metabolic state on intra-annual timescales (e.g. Champenois and Borges, 2012; Rheuban et al., 2014a, b). Here, we show that biotic components other than the seagrass itself can contribute to both the magnitude and variability in metabolic fluxes. Irrespective of traditional seagrass metrics such as seagrass shoot density and biomass, GPP and |CR| consistently increased in magnitude with meadow age which in turn corresponded to higher autotrophic diversity and macroalgal biomass. Further research should address whether these relationships are consistent across seasons and what role differing macrophyte phenologies play.

The chronosequence approach employed in this study utilizes the unique opportunity of assessing contrasting restored seagrass habitats of different ages that exist within a close distance from each other (Fig. 1). This enables comparisons between near-identical geomorphology, bathymetry, hydrodynamics and seawater characteristics. However, due to logistical limitations we were unable to measure all four sites simultaneously leading to a temporal mismatch of these comparisons. Consequently, this introduces the risk of potential environmental changes between deployments. Importantly, if the change in environmental conditions is conducive to altered benthic metabolism it can influence the comparison along the chronosequence (i.e between sites). The combined effect of abiotic variables, including PAR, flow velocity, seawater temperature and turbidity accounted for 20 % of the variation in O_2 fluxes, as measured by the eddy covariance. Noticeably, PAR reaching the seabed did not differ between sites, despite varying levels of turbidity (Fig. 2; Fig. S2). Salinity was higher in the 3 yr and Nat site compared to 7 yr and Bare (Table S2; Fig. S2). However, due to missing data, we could not evaluate its impacts on oxygen fluxes within the model. However, we found no discernable effects on either oxygen or carbon fluxes during our incubations, suggesting that variability in salinity was not a driving factor of metabolism. Flow velocity peaked in Nat and 7 yr sites but while there was a positive relationship between $|F_{O2}|$ and flow in Nat and 3 yr site, no such relationship was evident in the 7yr or Bare site (Fig. S3). Nonetheless, we cannot decisively rule out the potential role of varying flow velocities in the observed differences in benthic metabolism between sites.

Deleted: increased

Deleted:

Formatted: Subscript

Deleted: (Lindahl et al., 1998)

4.2 Carbon and oxygen balance

As part of this study, we present a methodological approach that estimates *in situ* DIC fluxes under natural hydrodynamic and light conditions. This is obtained by combining the advantages of aquatic eddy covariance with the ability to constrain the marine carbonate system and oxygen dynamics using benthic chambers. Concurrent deployment of these two methods have been utilized in previous coastal studies (Long et al., 2019; Camillini et al., 2021; Polsenaere et al., 2021), but only for comparing oxygen fluxes.

Assessing the *in situ* relationship between oxygen (F_{O2}) and DIC fluxes (F_{DIC}) can provide insights into biogeochemical processes and renders reliable estimates of photosynthetic (PQ) and respiratory quotients (RQ). All else equal, photosynthetic and respiratory quotients are governed by the C:N:P ratio of the fixed and respired organic matter present in the system (Champenois and Borges, 2021). However, considering the various sinks and sources of organic matter present in a seagrass meadow and the multitude of processes affecting F_{O2} and F_{DIC} differently, this is not very useful. Deviations from the theoretical 1:1 relationship between F_{O2} and F_{DIC} (Fig. 3d)

are thus ubiquitous in the literature (e.g. Barron et al., 2006; Turk et al., 2015; Trentman et al., 2023). In fact, the slope we observed is identical to what Pinardi et al. (2009) observed in sediments vegetated with the freshwater macrophyte *Vallisnera spiralis* using sediment cores. Moreover, our relatively low PQ's (0.34–0.52) were similar to what Ribaudo et al. (2011) observed in *V. spiralis* (0.30–0.68) in microcosms. The authors attributed the low PQ to oxygen transport to roots and subsequent radial oxygen loss (ROL) which fuels aerobic respiration, a process well-documented in *Z. marina* as well (e.g. Jensen et al., 2005; Frederiksen and Glud, 2006; Borum et al., 2007; Jovanovic et al., 2015). Turk et al. (2015) observed PQs ranging from 0.5–2.6 in seagrass (*Thallasia testudinium*) and found a temporal component to the variability of PQ with lower values in the morning and higher in the evening (Turk et al., 2015). Similar to our study, Ouisse et al. (2014) obtained a PQ and RQ of 0.42±0.27 and 0.95±0.22, respectively, using *in situ* benthic chambers in dwarf eelgrass (*Z. noltei*) meadows across several seasons. The authors hypothesized that the low PQ could also be due to photorespiration in epiphytic algae on the seagrass leaves which can consume more than three moles of O_2 for every mole DIC used (Ouisse et al., 2014). We observed large quantities of epiphytic microalgae and biofilm on seagrass leaves across all our studied meadows, albeit only as qualitative observations (Kindeberg, T., *pers. obs*.). However, seagrass epiphytes are abundant in the area where it can exert detrimental effects on seagrass metabolic performance and positive effects on epifauna distribution (Baden et al., 2010; Gullström et al., 2012; Brodersen et al., 2015). It is important to note that inorganic processes (i.e. $CaCO_3$ production and dissolution), which can have a large influence on PQ and RQ (Champenois and Borges, 2021), are implicitly accounted for in our F_{DIC} by subtraction of the $0.5F_{TA}$ term in Eq. (3).

While we obtained an average RQ close to unity, it was based on a relatively small sample size compared to PQ due to issues with dark incubations especially in the natural meadow. It is possible that our acclimation (~30 mins) or incubation times (3.0±0.1 hours) were too short for accurately capturing dark DIC fluxes, as seen in the temporal lag in DIC fluxes relative to O_2 fluxes in a study by Fenchel and Glud (2000) and a lag in O_2 consumption due to the primary producer cellular machinery (Tang and Kristensen, 2007). Nonetheless, without any ancillary data on other biogeochemical processes we cannot reconcile the sources of our observed PQ and RQ.

Deleted: *ii*

Deleted: Other biogeochemical processes such as production and consumption of highly oxidized photosynthates could be another explanation, but that is merely speculative at this stage and needs further research.

Deleted: ~3

4.3 Macrophyte diversity driving light-use efficiency and higher metabolism

Despite the large research field on the relationship between biodiversity and primary productivity (Tilman et al., 2014), light-use efficiency (LUE) is largely understudied in benthic metabolism studies (Attard and Glud, 2020). Studies have hitherto focused mainly on smaller-scale LUE, such as microalgae in microbial mats and corals (Al-Najjar et al., 2010; Al-Najjar et al., 2012; Brodersen et al., 2014). We observed a positive relationship between macrophyte diversity and LUE when controlling for biomass, indicating that mixed meadows consisting of both seagrass and macroalgae utilize light resources more efficiently and are more productive compared to monospecific meadows. Importantly, the restored seagrass meadows became more mixed over time as drifting macroalgae inhabited the meadow. These unattached algae are a common feature in the area, often considered a nuisance that can prevent seagrass recovery (Moksnes et al., 2018). Here it seems they also improve overall LUE of the meadow and contributes to larger metabolic fluxes.

Whether higher LUE is driven by certain species remains unclear, but the change in canopy structure and increasing three-dimensional complexity can positively influence LUE (Zimmerman, 2003; Binzer et al., 2006). Niche complementarity is common in ecological systems (Loreau and Hector, 2001; Hooper et al., 2005) and it is reasonable to believe that with increased diversity of autotrophs, pigment complementarity can facilitate optimal resource-use, especially as brown and red macroalgae are known to have a wide range of photosynthetic pigments (Enríquez et al., 1994). Additionally, the mere presence of multiple growth morphologies may induce self-shading that further increases LUE (Tait et al., 2014). An increase in photosynthetic pathways (e.g. C3 and C4) with higher macrophyte diversity and differing affinity for forms of inorganic nutrients (e.g. NH_4^+ and NO_3^-) is also expected. Moreover, both *Z. marina* and fucoid species are known to utilize both CO_2 and HCO_3^- for photosynthesis (Binzer et al., 2006). However, the efficiency differs between species (e.g. Larsson and Axelsson, 1999; Invers et al., 2001) and considering the large spatiotemporal variability in pH and $[HCO_3^-]$ relative to $[CO_2]$ we observed, this could be another reason for the higher LUE at higher species diversity. Studies from macroalgal canopies have found similar relationships between macrophyte canopy complexity and LUE, attributed to niche complementarity where intact assemblages are more efficient and productive than the sum of its parts (Tait and Schiel, 2011; Tait et al., 2014). For instance, a study by Tait and Schiel (2011) using *ex situ* incubation chambers found that an intact assemblage of seven species had higher net photosynthesis than the sum of all individual species. The authors observed that different species played different roles at different irradiances. For instance, the fucoid species *Cystophora torulosa* was exceptionally efficient at photosynthesizing at high irradiance and did not show signs of photoinhibition even at PAR > 2000 µmol m^{-2} s^{-1} (Tait and Schiel, 2011). Tait et al. (2014) studied P-I relationships in macroalgal assemblages and found that when more sub-canopy species where included (up to four) respiration and photosynthesis increased, thus corroborating our observed trends. However, they found that production did not saturate at incident irradiance of 2000 µmol m^2 s^{-1} as opposed to less speciose assemblages (2 sub-canopy species) that reached light saturation of net primary production (NPP) already at about 600 µmol m^2 s^{-1} (Tait et al., 2014). This is somewhat contrary to what we found for GPP, where P-I curves saturated at lower irradiance with higher macrophyte diversity (Fig. 5d; Fig. S6). Albeit not specifically addressing canopy structure or diversity, Rheuban et al. (2014a) found that a younger, five-year-old, restored *Z. marina* meadow was light-saturated while an older, 11-year-old meadow did not show any signs of light saturation, and this was consistent across seasons.

Deleted: 5

Whereas it is rather intuitive that a diverse community of primary producers are better at photosynthesizing (i.e. higher GPP), the relationship is as strong with CR. This is likely explained by the tight coupling between GPP and CR stemming from respiration of labile photosynthates (Penhale and Smith, 1977). However, detritus of macroalgae such as *Fucus* spp. is also more labile than *Z. marina*, partly due to a lower C:N ratio and a more bioavailable polysaccharide composition (e.g. Kristensen, 1994; Thomson et al., 2020).

4.4 The role of benthic diversity in seagrass metabolism

The fact that most fauna diversity metrics were not significantly different between the natural meadow and the youngest (3 yr) meadow implies that benthic diversity recovers quickly. Similar findings have recently been reported from *Z. marina* restoration projects in Denmark (Steinfurth et al., 2022) and from the very same sites as in this study (Gagnon et al., 2023). In fact, Gagnon et al. (2023) found that both taxonomic and functional diversity recovered within 15 months after restoration but already after 3 months the abundance was similar to documented

abundances in comparable seagrass meadows in the area. The authors partly attributed this to efficient larval dispersal from the adjacent natural meadow within the bay (Gagnon et al., 2023).

It is generally established that higher diversity yields higher productivity in seagrass meadows (Duffy et al., 2017), although the mechanisms behind the relationship are debated (Hooper et al., 2005; Gamfeldt et al., 2015). Based on our results, it seems that high macrophyte and macrofauna diversity positively influence GPP and CR, respectively, although the relationships with fauna are less clear. Aside from direct cellular respiration, many infauna species indirectly modify metabolic fluxes across the sediment-water interface through bioturbation and sediment reworking (Aller and Aller, 1998; Kristensen et al., 2012). A scrutiny of bioturbation and reworking modes revealed that especially biodiffusors and surficial modifiers increased with meadow age, despite highest total abundance of infauna in the youngest meadow (Table S4 & S6). It is possible that these functional modes benefited from larger quantities of macroalgal detritus building up on the sediment surface over the years. Thomson et al. (2020) found the lugworm *Arenicola marina*, an upward conveyor, contributed to a 37 % higher efflux of DIC in sediments containing *F. vesiculosus* compared to *Z. marina*. Macroalgal detritus was to a much higher extent respired or consumed compared to seagrass, which instead was buried in anoxic sediment layers by the lugworm (Thomson et al., 2020). Moreover, the role of bioturbation in oxygenating otherwise anoxic sediment can have large ramifications for sediment-water fluxes of DIC and could hence contribute to our observed CR.

Deleted: 2

Deleted: –

Deleted: 3

4.5 Implications of seagrass restoration on the carbon budget

The observed net heterotrophy during the productive season implies the system relies on either historic production of autochthonous carbon or on trophic subsidies to sustain metabolism. Albeit only covering a brief period within the summer season, our results suggest that the seagrass in this area receives large amounts of allochthonous carbon that is partly turned over and released as DIC. A large influx and sedimentation of allochthonous carbon was shown in a recent study by Dahl et al. (2023) from the same bay. They reported relatively high carbon accumulation rates (0.91±0.06 mol m^{-2} yr^{-1}) of which 51 % of sediment carbon originated from eelgrass productivity and 38 % from macroalgae (Dahl et al., 2023). Assuming this rate is constant throughout the year (0.0025 mol m^{-2} d^{-1}), this accumulation rate is about an order of magnitude lower than our measured summer NCP_{DIC}, implying that the majority of imported carbon is rapidly remineralized or assimilated by secondary producers (Fig. 7).

Our estimated budget of all carbon pools illustrates that whereas sediment stocks are the dominant pools, organic carbon is built up in living biomass following restoration (Table 4; Fig 7). Eelgrass and macroalgal biomass in the natural meadow made up 58 and 27 % of all biomass, respectively, which is on the same order as the relative proportion of sediment POC sources found in Dahl et al. (2023). Accumulation of sediment carbon and production of living biomass can be decoupled on longer time scales although trophic subsidies (i.e. external inputs) may be required to sustain both (Cebrian et al., 1997; Duarte et al., 2010; Huang et al., 2015). Notably, total fauna biomass also increased with meadow age, despite varying differences in abundance (Fig. 4; Fig. 7; Table S6).

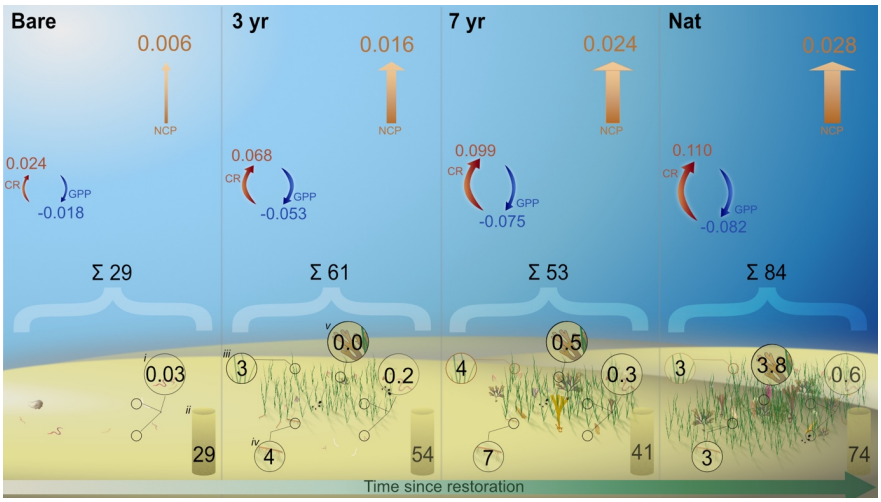

Figure 7 Pools and fluxes of carbon. Schematic illustration of a carbon budget including different benthic pools (mol C m^{-2}) of particulate organic carbon in i) fauna biomass, ii) sediment iii) eelgrass aboveground biomass, iv) eelgrass belowground biomass and v) macroalgal biomass. Arrows indicate the daily metabolic fluxes of dissolved inorganic carbon (mol m^{-2} d^{-1}) where blue arrows are gross primary productivity (GPP_{DIC}), red arrows are community respiration (CR_{DIC}) and orange arrows are net community productivity (NCP_{DIC}).

Deleted: **Tan and green arrows indicate lateral import and export of particulate organic carbon, respectively.**

While we are able to resolve the dominant carbon pools and metabolic fluxes, the import and export of organic carbon over seasonal timescales is required to reconcile the annual carbon cycling at this site. Nevertheless, it is reasonable to infer that NCP and carbon sequestration in these seagrass systems are sustained by lateral import of allochthonous organic carbon.

5. Conclusion

Planting seagrass initiates a profound transformation of the benthic environment that influences biodiversity and carbon cycling. Throughout our field study, we found that while fauna diversity developed in an anticipated successional pattern, the metabolic fluxes and net release of DIC were always higher in seagrass. These fluxes increased with meadow age and we observed increasing gross primary productivity and respiration as the seagrass grew and drifting algae and benthic fauna colonized. Collectively, our findings suggest a scenario where higher macrophyte and fauna diversity drives high primary productivity and respiration, respectively. Together with ample input of sestonic organic matter to this sheltered bay, these productive meadows act as effective bioreactors of organic carbon on diel timescales during summer, as evidenced by the net heterotrophic state and net efflux of DIC. These results highlight the intricate connections between carbon cycling and biodiversity that should be taken into consideration when restoring seagrass, especially in sheltered environments with large input of external organic matter. Yet, identifying the individual mechanisms and constraining the relative importance of fauna and flora diversity for benthic carbon fluxes remains a challenging task and should be a focal point in future research.

Deleted: is

Deleted: In this

Deleted: expected

Deleted: point to a plausible situation

Deleted: relationships

Deleted: separate

Deleted: difficult

Data availability

The dataset is freely available in the Zenodo repository (https://doi.org/10.5281/zenodo.8363551).

Author contributions

TK conceived the study with input from KMA, COQ and EI. TK, KMA, COQ and EI designed the field study. TK, KMA, JH, JM and EI conducted the field work. TK and KMA analyzed data. TK wrote the manuscript with input from all co-authors. All authors approved the submitted version of the article.

Conflict of interest statement

The authors declare that the research was conducted in the absence of any financial or commercial relationships that could be construed as potential conflicts of interest.

Acknowledgements

TK acknowledges funding from the Gyllenstiernska Krapperup Foundation (grant number KR2020-0066), the European Union LIFE programme (grant number LIFE17 CCA/SE/000048) and the Royal Physiographic Society of Lund (grant number 42518). KMA received funding from the Danish Institute for Advanced Study and COQ received funding from SDU Climate Cluster. We extend our gratitude to Dr. Florian Cesbron, Dr. Pierre Polsenaere and Dr. Guillaume Bernard whose constructive reviews significantly improved an earlier version of this manuscript. We thank Dr. Mogens Flindt for lending of benthic chambers, Dr. Adam Ulfsbo for assistance with total alkalinity analyses, Dr. Susanne Pihl Baden and Dr. Per Carlsson for help with fauna identification and Dr. Mirjam Victorin for assistance with flux calculations. We are also grateful for the hospitality and assistance of the staff at Kristineberg Center. Symbols used in figures courtesy of the Integration and Application Network, University of Maryland Center for Environmental Science.

References

Al-Najjar, M. A. A., de Beer, D., Kühl, M., and Polerecky, L.: Light utilization efficiency in photosynthetic microbial mats, Environmental microbiology, 14, 982-992, https://doi.org/10.1111/j.1462-2920.2011.02676.x, 2012.

Al-Najjar, M. A. A., de Beer, D., Jørgensen, B. B., Kühl, M., and Polerecky, L.: Conversion and conservation of light energy in a photosynthetic microbial mat ecosystem, The ISME Journal, 4, 440-449, https://doi.org/10.1038/ismej.2009.121, 2010.

Aller, R. C. and Aller, J. Y.: The effect of biogenic irrigation intensity and solute exchange on diagenetic reaction rates in marine sediments, Journal of Marine Research, 56, 905-936, https://doi.org/10.1357/002224098321667413, 1998.

Attard, K. M. and Glud, R. N.: Technical note: Estimating light-use efficiency of benthic habitats using underwater O2 eddy covariance, Biogeosciences, 17, 4343-4353, https://doi.org/10.5194/bg-17-4343-2020, 2020.

Attard, K. M., Rodil, I. F., Glud, R. N., Berg, P., Norkko, J., and Norkko, A.: Seasonal ecosystem metabolism across shallow benthic habitats measured by aquatic eddy covariance, Limnology and Oceanography Letters, 4, 75-86, https://doi.org/10.1002/lol2.10107, 2019.

Baden, S., Boström, C., Tobiasson, S., Arponen, H., and Moksnes, P.-O.: Relative importance of trophic interactions and nutrient enrichment in seagrass ecosystems: A broad-scale field experiment in the Baltic− Skagerrak area, Limnology and Oceanography, 55, 1435-1448, https://doi.org/10.4319/lo.2010.55.3.1435, 2010.

Barron, C., Duarte, C. M., Frankignoulle, M., and Borges, A. V.: Organic carbon metabolism and carbonate dynamics in a Mediterranean seagrass (Posidonia oceanica) meadow, Estuaries and Coasts, 29, 417-426, https://doi.org/10.1007/BF02784990, 2006.

Bates, D., Mächler, M., Bolker, B., and Walker, S.: Fitting Linear Mixed-Effects Models Using lme4, Journal of Statistical Software, 67, 1 - 48, https://doi.org/10.18637/jss.v067.i01, 2015.

Berg, P., Huettel, M., Glud, R. N., Reimers, C. E., and Attard, K. M.: Aquatic Eddy Covariance: The Method and Its Contributions to Defining Oxygen and Carbon Fluxes in Marine Environments, Annual Review of Marine Science, 14, 431-455, https://doi.org/10.1146/annurev-marine-042121-012329, 2022.

Berg, P., Delgard, M. L., Polsenaere, P., McGlathery, K. J., Doney, S. C., and Berger, A. C.: Dynamics of benthic metabolism, O2, and pCO2 in a temperate seagrass meadow, Limnology and Oceanography, 0, https://doi.org/10.1002/lno.11236, 2019.

Berg, P., Røy, H., Janssen, F., Meyer, V., Jørgensen, B. B., Huettel, M., and de Beer, D.: Oxygen uptake by aquatic sediments measured with a novel non-invasive eddy-correlation technique, Marine Ecology Progress Series, 261, 75-83, http://dx.doi.org/10.3354/meps261075, 2003.

Binzer, T., Sand-Jensen, K., and Middelboe, A.-L.: Community photosynthesis of aquatic macrophytes, Limnology and Oceanography, 51, 2722-2733, https://doi.org/10.4319/lo.2006.51.6.2722, 2006.

Borum, J., Sand-Jensen, K., Binzer, T., Pedersen, O., and Greve, T. M.: Oxygen movement in seagrasses, in: Seagrasses: Biology, ecology and conservation, edited by: Larkum, A. W. D., Orth, R. J., and Duarte, C. M., Springer, Dordrecht, 255-270, https://doi.org/10.1007/978-1-4020-2983-7, 2007.

Brodersen, K. E., Lichtenberg, M., Paz, L.-C., and Kühl, M.: Epiphyte-cover on seagrass (Zostera marina L.) leaves impedes plant performance and radial O2 loss from the below-ground tissue, Frontiers in Marine Science, 2, 58, https://doi.org/10.3389/fmars.2015.00058, 2015.

Brodersen, K. E., Lichtenberg, M., Ralph, P. J., Kühl, M., and Wangpraseurt, D.: Radiative energy budget reveals high photosynthetic efficiency in symbiont-bearing corals, Journal of The Royal Society Interface, 11, 20130997, https://doi.org/10.1098/rsif.2013.0997, 2014.
Camillini, N., Attard, K. M., Eyre, B. D., and Glud, R. N.: Resolving community metabolism of eelgrass Zostera marina meadows by benthic flume-chambers and eddy covariance in dynamic coastal environments, Marine Ecology Progress Series, 661, 97-114, https://doi.org/10.3354/meps13616, 2021.
Cebrian, J., Duarte, C. M., Marbà, N., and Enriquez, S.: Magnitude and fate of the production of four co-occurring western Mediterranean seagrass species, Marine Ecology Progress Series, 155, 29-44, https://doi.org/10.3354/meps155029, 1997.
Champenois, W. and Borges, A. V.: Seasonal and interannual variations of community metabolism rates of a Posidonia oceanica seagrass meadow, Limnology and Oceanography, 57, 347-361, https://doi.org/10.4319/lo.2012.57.1.0347, 2012.
Champenois, W. and Borges, A. V.: Net community metabolism of a Posidonia oceanica meadow, Limnology and Oceanography, 66, https://doi.org/10.1002/lno.11724, 2021.
Chevenet, F., Dolédec, S., and Chessel, D.: A fuzzy coding approach for the analysis of long-term ecological data, Freshwater Biology, 31, 295-309, https://doi.org/10.1111/j.1365-2427.1994.tb01742.x, 1994.
Dahl, M., Asplund, M. E., Bergman, S., Björk, M., Braun, S., Löfgren, E., Martí, E., Masque, P., Svensson, R., and Gullström, M.: First assessment of seagrass carbon accumulation rates in Sweden: A field study from a fjord system at the Skagerrak coast, PLOS Climate, 2, e0000099, https://doi.org/10.1371/journal.pclm.0000099, 2023.
Duarte, C. M.: Seagrass nutrient content, Marine Ecology Progress Series, 201-207, https://doi.org/10.3354/meps067201, 1990.
Duarte, C. M. and Cebrian, J.: The fate of marine autotrophic production, Limnology and Oceanography, 41, 1758-1766, https://doi.org/10.4319/lo.1996.41.8.1758, 1996.
Duarte, C. M. and Krause-Jensen, D.: Export from Seagrass Meadows Contributes to Marine Carbon Sequestration, Frontiers in Marine Science, 4, https://doi.org/10.3389/fmars.2017.00013, 2017.
Duarte, C. M., Sintes, T., and Marbà, N.: Assessing the CO2 capture potential of seagrass restoration projects, Journal of Applied Ecology, 50, 1341-1349, https://doi.org/10.1111/1365-2664.12155, 2013.
Duarte, C. M., Marbà, N., Gacia, E., Fourqurean, J. W., Beggins, J., Barron, C., and Apostolaki, E. T.: Seagrass community metabolism: Assessing the carbon sink capacity of seagrass meadows, Global Biogeochemical Cycles, 24, 8, https://doi.org/10.1029/2010gb003793, 2010.
Duffy, J. E., Godwin, C. M., and Cardinale, B. J.: Biodiversity effects in the wild are common and as strong as key drivers of productivity, Nature, 549, 261-264, https://doi.org/10.1038/nature23886, 2017.
Enríquez, S., Agustí, S., and Duarte, C. M.: Light absorption by marine macrophytes, Oecologia, 98, 121-129, https://doi.org/10.1007/BF00341462, 1994.
Faulwetter, S., Markantonatou, V., Pavloudi, C., Papageorgiou, N., Keklikoglou, K., Chatzinikolaou, E., Pafilis, E., Chatzigeorgiou, G., Vasileiadou, K., Dailianis, T., Fanini, L., Koulouri, P., and Arvanitidis, C.: Polytraits: A database on biological traits of marine polychaetes, Biodiversity Data Journal, 2, e1024, https://doi.org/10.3897/BDJ.2.e1024, 2014.
Fenchel, T. and Glud, R. N.: Benthic primary production and O2-CO2 dynamics in a shallow-water sediment: Spatial and temporal heterogeneity, Ophelia, 53, 159-171, https://doi.org/10.1080/00785236.2000.10409446, 2000.
Frederiksen, M. S. and Glud, R. N.: Oxygen dynamics in the rhizosphere of Zostera marina: A two-dimensional planar optode study, Limnology and Oceanography, 51, 1072-1083, https://doi.org/10.4319/lo.2006.51.2.1072 2006.

Gagnon, K., Bocoum, E.-H., Chen, C. Y., Baden, S. P., Moksnes, P.-O., and Infantes, E.: Rapid faunal colonization and recovery of biodiversity and functional diversity following eelgrass restoration, Restoration Ecology, 31, e13887, https://doi.org/10.1111/rec.13887, 2023.
Gamfeldt, L., Lefcheck, J. S., Byrnes, J. E. K., Cardinale, B. J., Duffy, J. E., and Griffin, J. N.: Marine biodiversity and ecosystem functioning: what's known and what's next?, Oikos, 124, 252-265, https://doi.org/10.1111/oik.01549, 2015.
Gattuso, J.-P., Epitalon, J.-M., Lavigne, H., and Orr, J. C.: seacarb: Seawater carbonate chemistry. R package version 3.3. https://cran.r-project.org/web/packages/seacarb/index.html [code], 2022.
Gattuso, J.-P., Magnan, A. K., Bopp, L., Cheung, W. W., Duarte, C. M., Hinkel, J., Mcleod, E., Micheli, F., Oschlies, A., and Williamson, P.: Ocean solutions to address climate change and its effects on marine ecosystems, Frontiers in Marine Science, 5, 337, https://doi.org/0.3389/fmars.2018.00337, 2018.
Glud, R. N.: Oxygen dynamics of marine sediments, Marine Biology Research, 4, 243-289, https://doi.org/10.1080/17451000801888726, 2008.
Gullström, M., Baden, S., and Lindegarth, M.: Spatial patterns and environmental correlates in leaf-associated epifaunal assemblages of temperate seagrass (Zostera marina) meadows, Marine Biology, 159, 413-425, https://doi.org/10.1007/s00227-011-1819-z, 2012.
Hannides, A. K., Glazer, B. T., and Sansone, F. J.: Extraction and quantification of microphytobenthic Chl a within calcareous reef sands, Limnology and Oceanography: methods, 12, 126-138, https://doi.org/10.4319/lom.2014.12.126, 2014.
Hooper, D. U., Chapin, F., Ewel, J., Hector, A., Inchausti, P., Lavorel, S., Lawton, J., Lodge, D., Loreau, M., and Naeem, S.: Effects of biodiversity on ecosystem functioning: a consensus of current knowledge, Ecological monographs, 75, 3-35, 2005.
Huang, Y.-H., Lee, C.-L., Chung, C.-Y., Hsiao, S.-C., and Lin, H.-J.: Carbon budgets of multispecies seagrass beds at Dongsha Island in the South China Sea, Marine Environmental Research, 106, 92-102, https://doi.org/10.1016/j.marenvres.2015.03.004, 2015.
Huber, S., Hansen, L. B., Nielsen, L. T., Rasmussen, M. L., Sølvsteen, J., Berglund, J., Paz von Friesen, C., Danbolt, M., Envall, M., Infantes, E., and Moksnes, P.: Novel approach to large-scale monitoring of submerged aquatic vegetation: A nationwide example from Sweden, Integrated Environmental Assessment and Management, 18, 909-920, https://doi.org/10.1002/ieam.4493, 2022.
Hume, A. C., Berg, P., and McGlathery, K. J.: Dissolved oxygen fluxes and ecosystem metabolism in an eelgrass (Zostera marina) meadow measured with the eddy correlation technique, Limnology and Oceanography, 56, 86-96, https://doi.org/10.4319/lo.2011.56.1.0086, 2011.
Infantes, E., Hoeks, S., Adams, M. P., van der Heide, T., van Katwijk, M. M., and Bouma, T. J.: Seagrass roots strongly reduce cliff erosion rates in sandy sediments, Marine Ecology Progress Series, 700, 1-12, https://doi.org/10.3354/meps14196, 2022.
Invers, O., Zimmerman, R. C., Alberte, R. S., Pérez, M., and Romero, J.: Inorganic carbon sources for seagrass photosynthesis: An experimental evaluation of bicarbonate use in species inhabiting temperate waters, Journal of Experimental Marine Biology and Ecology, 265, 203-217, https://doi.org/10.1016/S0022-0981(01)00332-X, 2001.
Jassby, A. D. and Platt, T.: Mathematical formulation of the relationship between photosynthesis and light for phytoplankton, Limnology and Oceanography, 21, 540-547, https://doi.org/10.4319/lo.1976.21.4.0540, 1976.
Jensen, S. I., Kühl, M., Glud, R. N., Jørgensen, L. B., and Priemé, A.: Oxic microzones and radial oxygen loss from roots of Zostera marina, Marine Ecology Progress Series, 293, 49-58, https://doi.org/10.3354/meps293049, 2005.

Jost, L.: Entropy and diversity, Oikos, 113, 363-375, https://doi.org/10.1111/j.2006.0030-1299.14714.x, 2006.
Jovanovic, Z., Pedersen, M. Ø., Larsen, M., Kristensen, E., and Glud, R. N.: Rhizosphere O2 dynamics in young Zostera marina and Ruppia maritima, Marine Ecology Progress Series, 518, 95-105, https://doi.org/10.3354/meps11041, 2015.
Kindeberg, T., Severinson, J., and Carlsson, P.: Eelgrass meadows harbor more macrofaunal species but bare sediments can be as functionally diverse, Journal of Experimental Marine Biology and Ecology, 554, 151777, https://doi.org/10.1016/j.jembe.2022.151777, 2022.
Kristensen, E.: Decomposition of macroalgae, vascular plants and sediment detritus in seawater: Use of stepwise thermogravimetry, Biogeochemistry, 26, 1-24, https://doi.org/10.1007/BF02180401, 1994.
Kristensen, E., Penha-Lopes, G., Delefosse, M., Valdemarsen, T., Quintana, C. O., and Banta, G. T.: What is bioturbation? The need for a precise definition for fauna in aquatic sciences, Marine Ecology Progress Series, 446, 285-302, https://doi.org/10.3354/meps09506, 2012.
Laliberté, E. and Legendre, P.: A distance-based framework for measuring functional diversity from multiple traits, Ecology, 91, 299-305, https://doi.org/10.1890/08-2244.1, 2010.
Larsson, C. and Axelsson, L.: Bicarbonate uptake and utilization in marine macroalgae, European Journal of Phycology, 34, 79-86, https://doi.org/10.1080/09670269910001736112, 1999.
Lindahl, O., Belgrano, A., Davidsson, L., and Hernroth, B.: Primary production, climatic oscillations, and physico-chemical processes: the Gullmar Fjord time-series data set (1985–1996), Ices Journal of Marine Science, 55, 723-729, 10.1006/jmsc.1998.0379, 1998.
Long, M. H., Rheuban, J. E., McCorkle, D. C., Burdige, D. J., and Zimmerman, R. C.: Closing the oxygen mass balance in shallow coastal ecosystems, Limnology and Oceanography, 0, https://doi.org/10.1002/lno.11248, 2019.
Loreau, M. and Hector, A.: Partitioning selection and complementarity in biodiversity experiments, Nature, 412, 72-76, https://doi.org/10.1038/35083573, 2001.
Lüdecke, D., Makowski, D., Waggoner, P., and Patil, I.: Performance: Assessment of regression models performance, R package version 0.4, 5, 2020.
Lueker, T. J., Dickson, A. G., and Keeling, C. D.: Ocean pCO(2) calculated from dissolved inorganic carbon, alkalinity, and equations for K-1 and K-2: validation based on laboratory measurements of CO2 in gas and seawater at equilibrium, Marine Chemistry, 70, 105-119, https://doi.org/10.1016/s0304-4203(00)00022-0, 2000.
The Marine Life Information Network: www.marlin.ac.uk, last access: 2022-10-15.
Mason, N. W., Mouillot, D., Lee, W. G., and Wilson, J. B.: Functional richness, functional evenness and functional divergence: the primary components of functional diversity, Oikos, 111, 112-118, https://doi.org/10.1111/j.0030-1299.2005.13886.x, 2005.
McGinnis, D. F., Sommer, S., Lorke, A., Glud, R. N., and Linke, P.: Quantifying tidally driven benthic oxygen exchange across permeable sediments: An aquatic eddy correlation study, Journal of Geophysical Research: Oceans, 119, 6918-6932, https://doi.org/10.1002/2014JC010303, 2014.
McGlathery, K. J., Reynolds, L. K., Cole, L. W., Orth, R. J., Marion, S. R., and Schwarzschild, A.: Recovery trajectories during state change from bare sediment to eelgrass dominance, Marine Ecology Progress Series, 448, 209-221, https://doi.org/10.3354/meps09574, 2012.
McKenzie, L. J., Nordlund, L. M., Jones, B. L., Cullen-Unsworth, L. C., Roelfsema, C., and Unsworth, R. K.: The global distribution of seagrass meadows, Environmental Research Letters, 074041, https://doi.org/10.1088/1748-9326/ab7d06, 2020.
Moksnes, P.-O., Eriander, L., Infantes, E., and Holmer, M.: Local Regime Shifts Prevent Natural Recovery and Restoration of Lost Eelgrass Beds Along the Swedish West Coast, Estuaries and Coasts, 1-20, https://doi.org/10.1007/s12237-018-0382-y, 2018.

Oksanen, J., Blanchet, G., Friendly, M., Klindt, R., Legendre, P., McGlinn, D., Minchin, P., O'Hara, G., Simpson, G., Solymos, P., Stevens, H., Szoecs, E., and Wagner, H.: vegan: Community Ecology Package R. https://cran.r-project.org/web/packages/vegan/index.html [code], 2019.
Olsson, J., Toth, G. B., and Albers, E.: Biochemical composition of red, green and brown seaweeds on the Swedish west coast, Journal of Applied Phycology, 32, 3305-3317, https://doi.org/10.1007/s10811-020-02145-w, 2020.
Orth, R. J., Lefcheck, J. S., McGlathery, K. S., Aoki, L., Luckenbach, M. W., Moore, K. A., Oreska, M. P. J., Snyder, R., Wilcox, D. J., and Lusk, B.: Restoration of seagrass habitat leads to rapid recovery of coastal ecosystem services, Science Advances, 6, eabc6434, https://doi.org/10.1126/sciadv.abc6434, 2020.
Österling, M. and Pihl, L.: Effects of filamentous green algal mats on benthic macrofaunal functional feeding groups, Journal of Experimental Marine Biology and Ecology, 263, 159-183, https://doi.org/10.1016/S0022-0981(01)00304-5, 2001.
Ouisse, V., Migné, A., and Davoult, D.: Comparative study of methodologies to measure in situ the intertidal benthic community metabolism during immersion, Estuarine, Coastal and Shelf Science, 136, 19-25, https://doi.org/10.1016/j.ecss.2013.10.032, 2014.
Penhale, P. A. and Smith, W. O.: Excretion of dissolved organic carbon by eelgrass (Zostera marina) and its epiphytes, Limnology and Oceanography, 22, 400-407, https://doi.org/10.4319/lo.1977.22.3.0400, 1977.
Pinardi, M., Bartoli, M., Longhi, D., Marzocchi, U., Laini, A., Ribaudo, C., and Viaroli, P.: Benthic metabolism and denitrification in a river reach: a comparison between vegetated and bare sediments, Journal of Limnology, 68, 133-145, https://doi.org/10.4081/jlimnol.2009.133, 2009.
Platt, T., Gallegos, C. L., and Harrison, W. G.: Photoinhibition of photosynthesis in natural assemblages of marine phytoplankton, Journal of Marine Research, 38, 687-701, 1980.
Polsenaere, P., Deflandre, B., Thouzeau, G., Rigaud, S., Cox, T., Amice, E., Bec, T. L., Bihannic, I., and Maire, O.: Comparison of benthic oxygen exchange measured by aquatic Eddy Covariance and Benthic Chambers in two contrasting coastal biotopes (Bay of Brest, France), Regional Studies in Marine Science, 43, 101668, https://doi.org/10.1016/j.rsma.2021.101668, 2021.
Queirós, A. M., Birchenough, S. N., Bremner, J., Godbold, J. A., Parker, R. E., Romero-Ramirez, A., Reiss, H., Solan, M., Somerfield, P. J., and Van Colen, C.: A bioturbation classification of European marine infaunal invertebrates, Ecology and evolution, 3, 3958-3985, https://doi.org/10.1002/ece3.769, 2013.
RCoreTeam: R: A Language and Environment for Statistical Computing, R Foundation for Statistical Computing [code], 2023.
Remy, F., Michel, L. N., Mascart, T., De Troch, M., and Lepoint, G.: Trophic ecology of macrofauna inhabiting seagrass litter accumulations is related to the pulses of dead leaves, Estuarine, Coastal and Shelf Science, 252, 107300, https://doi.org/10.1016/j.ecss.2021.107300, 2021.
Rheuban, J. E., Berg, P., and McGlathery, K. J.: Ecosystem metabolism along a colonization gradient of eelgrass (Zostera marina) measured by eddy correlation, Limnology and Oceanography, 59, 1376-1387, https://doi.org/10.4319/lo.2014.59.4.1376, 2014a.
Rheuban, J. E., Berg, P., and McGlathery, K. J.: Multiple timescale processes drive ecosystem metabolism in eelgrass (Zostera marina) meadows, Marine Ecology Progress Series, 507, 1-13, https://doi.org/10.3354/meps10843 2014b.
Ribaudo, C., Bartoli, M., Racchetti, E., Longhi, D., and Viaroli, P.: Seasonal fluxes of O2, DIC and CH4 in sediments with Vallisneria spiralis: indications for radial oxygen loss, Aquatic Botany, 94, 134-142, https://doi.org/10.1016/j.aquabot.2011.01.003, 2011.

Riera, R., Vasconcelos, J., Baden, S., Gerhardt, L., Sousa, R., and Infantes, E.: Severe shifts of Zostera marina epifauna: Comparative study between 1997 and 2018 on the Swedish Skagerrak coast, Marine pollution bulletin, 158, 111434, https://doi.org/10.1016/j.marpolbul.2020.111434, 2020.
Rodil, I. F., Attard, K. M., Gustafsson, C., and Norkko, A.: Variable contributions of seafloor communities to ecosystem metabolism across a gradient of habitat-forming species, Marine Environmental Research, 105321, https://doi.org/10.1016/j.marenvres.2021.105321, 2021.
Rodil, I. F., Attard, K. M., Norkko, J., Glud, R. N., and Norkko, A.: Towards a sampling design for characterizing habitat-specific benthic biodiversity related to oxygen flux dynamics using Aquatic Eddy Covariance, PLoS One, 14, e0211673, https://doi.org/10.1371/journal.pone.0211673, 2019.
Rodil, I. F., Attard, K. M., Norkko, J., Glud, R. N., and Norkko, A.: Estimating Respiration Rates and Secondary Production of Macrobenthic Communities Across Coastal Habitats with Contrasting Structural Biodiversity, Ecosystems, 23, 630-647, https://doi.org/10.1007/s10021-019-00427-0, 2020.
Rodil, I. F., Lohrer, A. M., Attard, K. M., Thrush, S. F., and Norkko, A.: Positive contribution of macrofaunal biodiversity to secondary production and seagrass carbon metabolism, Ecology, e3648, 2022.
Smith, S. V. and Hollibaugh, J. T.: Coastal metabolism and the oceanic organic carbon balance, Reviews of Geophysics, 31, 75-89, https://doi.org/10.1029/92rg02584, 1993.
Smith, S. V. and Key, G. S.: Carbon dioxide and metabolism in marine environments, Limnology and Oceanography, 20, 493-495, https://doi.org/10.4319/lo.1975.20.3.0493, 1975.
Steinfurth, R. C., Lange, T., Oncken, N. S., Kristensen, E., Quintana, C. O., and Flindt, M. R.: Improved benthic fauna community parameters after large-scale eelgrass (Zostera marina) restoration in Horsens Fjord, Denmark, Marine Ecology Progress Series, 687, 65-77, https://doi.org/10.3354/meps14007, 2022.
Sundbäck, K., Linares, F., Larson, F., Wulff, A., and Engelsen, A.: Benthic nitrogen fluxes along a depth gradient in a microtidal fjord: the role of denitrification and microphytobenthos, Limnology and Oceanography, 49, 1095-1107, 2004.
Tait, L. W. and Schiel, D. R.: Dynamics of productivity in naturally structured macroalgal assemblages: importance of canopy structure on light-use efficiency, Marine Ecology Progress Series, 421, 97-107, https://doi.org/10.3354/meps08909, 2011.
Tait, L. W., Hawes, I., and Schiel, D. R.: Shining Light on Benthic Macroalgae: Mechanisms of Complementarity in Layered Macroalgal Assemblages, PLoS One, 9, e114146, https://doi.org/10.1371/journal.pone.0114146, 2014.
Tang, M. and Kristensen, E.: Impact of microphytobenthos and macroinfauna on temporal variation of benthic metabolism in shallow coastal sediments, Journal of Experimental Marine Biology and Ecology, 349, 99-112, https://doi.org/10.1016/j.jembe.2007.05.011, 2007.
Thomson, A. C. G., Kristensen, E., Valdemarsen, T., and Quintana, C. O.: Short-term fate of seagrass and macroalgal detritus in Arenicola marina bioturbated sediments, Marine Ecology Progress Series, 639, 21-35, https://doi.org/10.3354/meps13281 2020.
Tilman, D., Isbell, F., and Cowles, J. M.: Biodiversity and Ecosystem Functioning, Annual Review of Ecology, Evolution, and Systematics, 45, 471-493, https://doi.org/10.1146/annurev-ecolsys-120213-091917, 2014.
Törnroos, A. and Bonsdorff, E.: Developing the multitrait concept for functional diversity: lessons from a system rich in functions but poor in species, Ecological Applications, 22, 2221-2236, https://doi.org/10.1890/11-2042.1, 2012.
Trentman, M. T., Hall Jr., R. O., and Valett, H. M.: Exploring the mismatch between the theory and application of photosynthetic quotients in aquatic ecosystems, Limnology and Oceanography Letters, 8, 565-579, https://doi.org/10.1002/lol2.10326, 2023.

Turk, D., Yates, K. K., Vega-Rodriguez, M., Toro-Farmer, G., L'Esperance, C., Melo, N., Ramsewak, D., Dowd, M., Estrada, S. C., Muller-Karger, F. E., Herwitz, S. R., and McGillis, W. R.: Community metabolism in shallow coral reef and seagrass ecosystems, lower Florida Keys, Marine Ecology Progress Series, 538, 35-52, https://doi.org/10.3354/meps11385, 2015.
Unsworth, R. K. F., Cullen-Unsworth, L. C., Jones, B. L. H., and Lilley, R. J.: The planetary role of seagrass conservation, Science, 377, 609-613, https://doi.org/10.1126/science.abq6923, 2022.
Van Dam, B. R., Lopes, C., Osburn, C. L., and Fourqurean, J. W.: Net heterotrophy and carbonate dissolution in two subtropical seagrass meadows, Biogeosciences, 16, 4411-4428, https://doi.org/10.5194/bg-16-4411-2019, 2019.
Villéger, S., Mason, N. W., and Mouillot, D.: New multidimensional functional diversity indices for a multifaceted framework in functional ecology, Ecology, 89, 2290-2301, https://doi.org/10.1890/07-1206.1, 2008.
Ward, M., Kindinger, T. L., Hirsh, H. K., Hill, T. M., Jellison, B. M., Lummis, S., Rivest, E. B., Waldbusser, G. G., Gaylord, B., and Kroeker, K. J.: Reviews and syntheses: Spatial and temporal patterns in seagrass metabolic fluxes, Biogeosciences, 19, 689-699, https://doi.org/10.5194/bg-19-689-2022, 2022.
Waycott, M., Duarte, C. M., Carruthers, T. J. B., Orth, R. J., Dennison, W. C., Olyarnik, S., Calladine, A., Fourqurean, J. W., Heck, K. L., Hughes, A., Kendrick, G. A., Kenworthy, W., Short, F. T., and Williams, S. L.: Accelerating loss of seagrasses across the globe threatens coastal ecosystems, Proceedings of the National Academy of Sciences, USA, 106, 12377-12381, https://doi.org/10.1073/pnas.0905620106, 2009.
Weiss, R.: The solubility of nitrogen, oxygen and argon in water and seawater, Deep sea research and oceanographic abstracts, 721-735, https://doi.org/10.1016/0011-7471(70)90037-9,
Wijsman, J. W. M., Herman, P. M. J., and Gomoiu, M.-T.: Spatial distribution in sediment characteristics and benthic activity on the northwestern Black Sea shelf, Marine Ecology Progress Series, 181, 25-39, http://dx.doi.org/10.3354/meps181025, 1999.
Zimmerman, R. C.: A biooptical model of irradiance distribution and photosynthesis in seagrass canopies, Limnology and Oceanography, 48, 568-585, https://doi.org/10.4319/lo.2003.48.1_part_2.0568, 2003.